

CR 86328
N70-20428

Final Report

NON-INVASIVE, MULTICHROMATIC EYE OXIMETER

By

Ronald A. Laing
Lee A. Danisch
Laurence R. Young

October 1969

Distribution of this report is provided in the interest of information exchange and should not be construed as endorsement by NASA of the material presented. Responsibility for the contents resides with the organization that prepared it.

Prepared under Contract No. NAS 12-2018

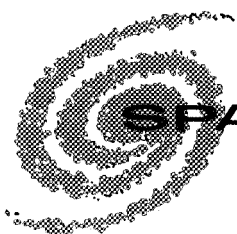
By

SPACE SCIENCES INCORPORATED
301 Bear Hill Road
Waltham, Massachusetts 02154

CASE FILE COPY

For

Electronics Research Center
NATIONAL AERONAUTICS AND SPACE ADMINISTRATION
575 Technology Square
Cambridge, Massachusetts 02159



SPACE SCIENCES INCORPORATED

301 BEAR HILL ROAD, WALTHAM, MASSACHUSETTS, 02154
A WHOLLY OWNED SUBSIDIARY OF WHITTAKER CORPORATION

Matthew J. Hillsman
Technical Monitor
NAS 12-2018
Electronics Research Center
575 Technology Square
Cambridge, Massachusetts 02139

Requests for copies of this report should be referred to:

NASA Scientific and Technical Information Facility
P.O. Box 33, College Park, Maryland 20740

FINAL REPORT

NON-INVASIVE, MULTICHROMATIC
EYE OXIMETER

By

Ronald A. Laing

Lee A. Danisch

Laurence R. Young

October 1969

Prepared under Contract No. NAS 12-2018

By

SPACE SCIENCES INCORPORATED

301 Bear Hill Road

Waltham, Massachusetts

For

Electronics Research Center

NATIONAL AERONAUTICS AND SPACE ADMINISTRATION

575 Technology Square

Cambridge, Massachusetts

SUMMARY

The Eye Oximeter is an electro-optical instrument that non-invasively measures the oxygen saturation of choroidal blood in the back of the eye. The spectrophotometric method used by the Eye Oximeter is similar to that used in standard cuvette reflection oximeters such as the American Optical. The instrument consists of two basic systems: the Optical System and the Electronic System. The Optical System produces a suitable multi-chromatic beam of light, reflects this beam from the fundus of the subject's eye, and onto a low-noise photodetector. The Electronic System amplifies the weak composite signal from the photodetector, separates the two spectral components, computes the average oxygen saturation from the area of the fundus that was sampled, and displays the value of the computed oxygen saturation on a panel meter. The instrument may be used with an external chart recorder to continuously record kinetic changes of either the oxygen saturation or the fundus reflectivity at each of the two measuring wavelengths. Since choroidal blood is characteristic of blood which is supplied to the brain, the Eye Oximeter is essentially using the eye as a "window" to look into the brain. The instrument can thus be used to monitor the amount of oxygen which is supplied to the brain under varying external conditions.

TABLE OF CONTENTS

<u>Section</u>		<u>Page</u>
	SUMMARY	ii
	LIST OF FIGURES	iv
	LIST OF TABLES	v
	LIST OF SYMBOLS	vi
1	INTRODUCTION	1
2	PHYSIOLOGICAL SIGNIFICANCE AND BASIC THEORY OF THE MEASUREMENT	3
3	DESCRIPTION OF THE EYE OXIMETER	8
	3.1 The Optical System	11
	3.2 The Electronic System	17
4	OPERATION OF THE INSTRUMENT	33
	4.1 Preliminary Calibration and Adjustment of the Electronics	33
	4.2 Observation of the Fundus	39
	4.3 Final Adjustment of the Electronics and Calibration of the Eye Oximeter	42
5	PERFORMANCE OF THE EYE OXIMETER	44
	REFERENCES	52
	APPENDICES	
	A. Theory of the Eye Oximeter	53
	B. Calculation of the Eye Oximeter Signal-to-Noise Ratio	63
	C. New Technology Appendix	76

LIST OF FIGURES

<u>Figure</u>		<u>Page</u>
1	The Eye Oximeter	9
2	The Multi-Chromatic Eye Oximeter	10
3	Optical Layout Diagram of DBLS	12
4	Transmission Curves for DM1 and DM2	13
5	Optical Diagram of Fundus Monitoring Unit	14
6	Block Diagram of Electronic Circuitry for Oximeter	18
7	Schematic Diagram of FCS Lamp Power Supply and Light Monitor	19
8	Schematic Diagram of Electronics in Fundus Monitor	24
9	Relay Rack	26
10	Schematic Diagram of Computation Circuitry Module	29
11	Fundus Monitoring Unit	36
12	Illumination Diaphragms	40
13	Iris Diaphragm Image	40
14	Calculated Oxygen Saturation vs Time for Changes in Breathing Mixture	45
15	Correlation of Oxygen Saturation Changes with Breathing	46
16	Artifacts and Spurious Responses	48
17	Computed Oxygen Saturation vs. Time for a Trained Fatigued Subject	49
18	Oxygen Saturation vs. Breathing Mixture for a Fatigued Subject	50
19	Stability of the Eye Oximeter	51
A-1	The Human Eye	54
A-2	Model of the Fundus	56
B-1	Optical Layout Diagram of DBLS	64

LIST OF TABLES

<u>Table</u>		<u>Page</u>
I	Schedule of Cable Connections	21
B-I	Summary of Results	65

LIST OF SYMBOLS

a	function of extinction coefficients at wavelengths used for reflection measurement
b	function of extinction coefficients at wavelengths used for reflection measurements
$c = c_{\text{Hb}} + c_{\text{HbO}_2}$	total hemoglobin concentration of a given blood sample
c_{Hb}	hemoglobin concentration of a given blood sample
c_{HbO_2}	oxyhemoglobin concentration of a given blood sample
d	diameter
f	focal length
ℓ	reflection loss
n	index of refraction
x	distance into choroid from front surface
A	area
A_T	function of extinction coefficients at wavelengths used for transmission measurement
B_T	function of extinction coefficients of wavelengths used for transmission measurement
C_1	first radiation constant
C_2	second radiation constant
$D(\lambda)$	optical density as a function of wavelength
Hb	hemoglobin
HbO_2	oxyhemoglobin
$I_B = I_B(x)$	intensity of light scattered in the backward direction in passing through a layer of blood of thickness dx located at a distance x from the front surface of the choroid
$I_F = I_F(x)$	intensity of light scattered in the forward direction in passing through a layer of blood of thickness dx located at a distance x from the front surface of the choroid

$I_o = I_o(\lambda)$	intensity of light of wavelength λ incident upon the choroid
$I_R = I_R(\lambda)$	intensity of light of wavelength λ diffusely reflected from the choroid
$I_T = I_T(x)$	intensity of light transmitted in the forward direction at a distance x from the front surface of the choroid
K	ratio of illuminated to effective area
$P_D(\lambda)$	radiant flux incident on photodetector, within band centered at λ
$P_Q(\lambda)$	radiant flux from source, within band centered at λ
R	reflection coefficient
$S = \frac{C_{HbO_2}}{C_{Hb} + C_{HbO_2}}$	oxygen saturation of blood
S_R	oxygen saturation measured by reflection technique
S_T	oxygen saturation measured by transmission technique
S/N	signal-to-noise ratio
T	absolute temperature
T_i	transmission coefficient of element i of optical system
T_o	collection efficiency
W	total radiant emittance
$W(\lambda)$	radiant emittance within the band centered at λ
α	proportionality factor
β	proportionality factor
γ	observed (effective) area
ϵ	emissivity
θ	illuminated area
λ	wavelength
μ	molecular absorption coefficient of blood
μ_{Hb}	molecular absorption coefficient of hemoglobin

μ_{HbO_2}	molecular absorption coefficient of oxyhemoglobin
σ	Stefan-Boltzmann constant
σ_{B}	backward scattering coefficient of blood
σ_{F}	forward scattering coefficient of blood
ϕ	angle of incidence
ϕ^1	angle of refraction
Φ	radiant flux
Ω	solid angle

Final Report

Non-Invasive, Multichromatic Eye Oximeter

By

Ronald A. Laing, Lee A. Danisch and Laurence R. Young

Space Sciences Incorporated
Waltham, Massachusetts

1. INTRODUCTION

The Eye Oximeter is an electro-optical instrument that measures the oxygen saturation of blood in the back of the eye. The measurement is made non-invasively by shining a multichromatic beam of light into the eye and measuring the amount of light of each of two spectral components which is reflected from the fundus. The light intensities which are used to make the measurement or to view the fundus prior to or during the measurement are sufficiently low that little or no discomfort is experienced by the subject.

Since choroidal blood is characteristic of blood which is supplied to the brain the Eye Oximeter is in a sense using the eye as a "window" to look into the brain. The instrument can thus be used to monitor the amount of oxygen which is supplied to the brain under varying external conditions. The brain is the most sensitive organ of the human body to oxygen starvation. As the oxygen saturation of cranial blood is lowered, faintness, visual and functional loss, unconsciousness, and finally death can result. Such a situation might arise for astronauts breathing a multigas cabin atmosphere should a system malfunction occur. In such instances the Eye Oximeter would be invaluable for periodically monitoring the cranial blood oxygen saturation. Such a measurement would permit an astronaut to manually regulate the amount of oxygen in the cabin gas to a level which, while being physiologically acceptable and safe would preserve the oxygen supply as much as possible.

The Eye Oximeter is also useful as a research instrument to study changes

of choroidal and cranial blood oxygen saturation resulting from changes of inspired gas mixtures, drugs, varying force fields, and trauma. Coupling the instrument with an external recorder allows kinetic changes of oxygen saturation and fundal reflectivity at 650 nm and 805 nm to be recorded simultaneously if desired. This enables physiological time constants associated with oxygen saturation changes to be studied and determined. Since the Eye Oximeter is the first instrument to allow a rapid and accurate measurement of choroidal oxygen saturation to be made, other applications and uses for the instrument will undoubtedly arise in the future.

The feasibility of an Eye Oximeter was originally shown by Broadfoot, Gloster, and Greaves (Ref. 1) who succeeded in obtaining reflected signals from the human fundus of red, yellow, and blue light obtained using colored glass filters. These authors showed in this and subsequent work (Ref. 2,3) that the fundal reflection coefficient of red light changed significantly when the subject's choroidal oxygen saturation was lowered by either nitrogen breathing or apnea following hyperventillation.

We would like to acknowledge Dr. Sol Aisenberg, Dr. David Sheena, Mr. Joel Newman, Mr. James E. Dodge and Mr. George Leonard for their advice and assistance during the technical design and development stage of the program. Thanks also to Mr. Peter Cardia and Mr. James Pratt for their technical assistance in the construction of the instrument. We would also like to acknowledge Miss Mary Ellen Dougall for her valuable services during all phases of the program including design and development and the preparation of reports.

2. PHYSIOLOGICAL SIGNIFICANCE AND BASIC THEORY OF THE MEASUREMENT

One of the prime functions of the blood is to transport oxygen from the lungs to the tissues where the oxygen is released and utilized as one of the required metabolites of living tissue cells. This oxygen transport is accomplished using the hemoglobin contained in the red blood cells as a carrier. As the venous blood passes through the pulmonary capillaries, oxygen, which has diffused through the alveolar endothelium, bonds to hemoglobin to form oxyhemoglobin. As the blood passes through the vascular beds of the various tissues this oxygen becomes dissociated from the oxyhemoglobin and passes through the tissue cell membrane where it is used as a metabolite. The hemoglobin is left in its reduced state and returns to the lung in the venous blood. Upon passing through the pulmonary vasculature again, the hemoglobin picks up additional oxygen to become oxyhemoglobin and the oxygen transport cycle starts over again.

The amount of oxygen bonded to the hemoglobin in a given quantity of blood is represented by the oxygen saturation, S , which is defined as:

$$S = \frac{c_{\text{HbO}_2}}{c_{\text{Hb}} + c_{\text{HbO}_2}}$$

where c_{HbO_2} and c_{Hb} are the concentrations of oxyhemoglobin and hemoglobin, respectively, in the given quantity of blood.

For a person breathing room air under normal conditions the oxygen saturation of arterial blood is approximately 97%. Due to certain conditions of stress or as a result of breathing a gas mixture which has a reduced gaseous oxygen concentration the arterial oxygen saturation can fall to lower levels than this. Should the arterial oxygen saturation fall to too low a

value, oxygen deprivation occurs since the tissues are unable to extract from the blood sufficient oxygen to satisfy their normal metabolic requirements. If the arterial oxygen saturation remains at such a low level, unconsciousness, tissue necrosis, and finally death will result.

The most sensitive organ of the body to oxygen deprivation is the brain. Elimination of blood flow, and the resulting oxygen starvation to the brain for only 4-5 minutes results in tissue necrosis and irreversible brain damage, while circulatory arrest for periods of greater than 10 minutes almost universally destroys most, if not all, of the mental powers. (Ref. 4) For the reduction of cranial arterial oxygen saturation, while maintaining a normal cranial blood flow rate, the results, if less abrupt, are no less striking and certain. As the cranial arterial oxygen saturation falls to approximately 93% central visual acuity, brightness contrast, and field extent are seriously impaired. (Ref. 5) Further reductions in saturation produce decrements in coordination, judgement, and memory, until at a level of approximately 60% collapse of the subject is imminent. Prolonged periods at this or lower levels of cranial arterial oxygen saturation would result in permanent brain damage and ultimately death.

Loss of functional ability to perform manual tasks would also occur as the arterial oxygen saturation fell, in parallel with the alterations in vision. As is well known, considerable functional ability has already been lost when subjective indications of low arterial oxygen saturation, such as dizziness and loss of visual field, have occurred. For astronauts or aquanauts living in an artificial environment, in which a system malfunction could reduce the oxygen concentration in the breathing mixture to a dangerous level, the unnoticed loss of functional ability could prevent the proper corrective measures from being taken to eliminate the malfunction after the subjective awareness of the difficulty occurred.

The spectrophotometric technique used by the Eye Oximeter is similar to that used by standard cuvette oximeters such as the American Optical. This technique depends for its validity upon the difference in molecular absorption coefficients of hemoglobin and oxyhemoglobin. The technique requires the use of two different wavelengths in order to provide a measurement which is independent of hematocrit and local variations in erythrocyte concentration. The Eye Oximeter uses 805 nm as one of the required wavelengths and 650 nm as the other. 805 nm is chosen since it is generally accepted as an isobestic wavelength (Ref. 6) for which the molecular absorption coefficients of Hb and HbO₂ are identical. The optical scattering properties of blood at this wavelength are thus independent of the local oxygen saturation and dependent only on the local hematocrit or total hemoglobin concentration. The other wavelength is more arbitrarily chosen as 650 nm and is a compromise between a wavelength having the maximum difference between the molecular absorption coefficients of Hb and HbO₂ and a wavelength at which the slopes of the molecular absorption coefficients of Hb and HbO₂ are both small. The optical scattering properties of blood at 650 nm are thus strongly dependent upon the oxygen saturation.

In practice two types of cuvette oximeters are used, transmission oximeters and reflection oximeters. In a typical transmission oximeter, light of the two wavelengths, 805 nm and 650 nm, is transmitted through a hemolyzed blood sample contained in a cuvette, and the optical density, $D(\lambda)$, is measured at each of the wavelengths. The oxygen saturation for such a transmission oximeter, S_T , is given in this case by the linear relationship (Ref. 7):

$$S_T = A_T \left[\frac{D(650)}{D(805)} \right] + B_T \quad (1)$$

where A_T and B_T are functions of the extinction coefficients at 650 and

805 nm. In the transmission method, hemolysis of the blood is necessary to eliminate artifacts associated with multiple scattering of the measuring light from the erythrocytes (Ref. 8, 9).

In a typical reflection oximeter the intensity of light diffusely reflected from a sample of unhemolyzed blood, $I_R(\lambda)$, is measured at two wavelengths. As is shown in Appendix A the oxygen saturation, S_R , for a reflection oximeter is given by the equation;

$$S_R = a \left[\frac{I_R(805)}{I_R(650)} \right] + b \quad (2)$$

where a and b are functions of the extinction coefficients at 650 and 805 nm (Ref.6).

In the Eye Oximeter it is not a priori evident whether a reflection or a transmission measurement is being made. When the measuring light is incident upon the cornea of the eye it passes through the cornea, aqueous humor, lens, and vitreous humor to the fundus. There it is transmitted through the retina and pigment epithelium to the choroid. As the measuring light passes down through the choroid, a fraction of it is diffusely reflected back out through the eye into the Eye Oximeter for measurement. If the diffusely reflected beam of light from the choroid were the only light which emanated from the eye, then the measurement would clearly be one of reflection. However, if the choroid is sufficiently thin, the transmitted light intensity at the choroid-sclera boundary can be non-zero. In this case the incident beam would be reflected by the sclera and retransmitted back through the choroid, and would emanate from the eye as a "transmitted" beam. Due to the thickness of the choroid (about 175μ , Ref. 10) and the diffusely reflecting nature of the sclera it would seem unlikely that an appreciable contribution to the emanated light would result as a result of

this doubly transmitted beam. If this is the case, the Eye Oximeter would then essentially make a reflection measurement of the choroidal oxygen saturation. Assuming this to be the case, and choosing an appropriate model of the choroid, a first order theory of the eye oximetry measurement has been worked out and is presented in Appendix A. This calculation shows that for a reflection method the equation giving the choroidal oxygen saturation has the same form as equation (2), as for the standard cuvette reflection oximeter. In addition, a straightforward modification of the calculation of Appendix A would show that for an assumed transmission method the equation giving the choroidal oxygen saturation has the same form as equation (1), as for the transmission cuvette oximeter.

Although the computational circuitry calculates the oxygen saturation from an equation equivalent to equation (2), the Eye Oximeter circuitry is easily modified to calculate whatever the proper function should turn out to be. Since the measuring beam of light emanating from the eye would be a linear combination of the reflected and transmitted components the most general equation to be calculated would be

$$S = \alpha S_T + \beta S_R \quad (3)$$

where α and β are constants, and S_T and S_R are given by equations (1) and (2) respectively. However, only when S_T and S_R were of comparable magnitudes would equation (3) need to be calculated. If α/β were small, most of the contribution to S would be due to the reflected beam. In this case S_R could be calculated by the computational circuitry and the meter face could be hand-calibrated to eliminate the small amount of non-linearity introduced by the transmitted beam.

3. DESCRIPTION OF THE EYE OXIMETER

Fig. 1 shows a photograph of the Eye Oximeter in operation. The instrument is conveniently divided into an Optical System and an Electronic System. The Optical System produces a suitable multi-chromatic beam of light, reflects this beam from the fundus of the subject's eye, and focuses the desired fraction of the light reflected from the fundus onto a photodetector. The Optical System also contains a viewing light of adjustable intensity which allows the subject's fundus to be observed by the operator when desired. The Electronic System amplifies the weak signal from the photodetector, computes the average oxygen saturation from that area of the fundus which was sampled, and displays the value of the computed oxygen saturation on a panel meter. Provision is also made for allowing the computed oxygen saturation and the reflected intensities of the two measuring wavelengths, 650 nm and 805 nm, to be recorded on an external strip chart recorder.

Figure 2 shows a block diagram of the Eye Oximeter. The specific function of each of the blocks shown is discussed in detail later in this section. As is seen in this figure, the Optical System consists of the Dual Beam Light Source (DBLS), the Fundus Monitoring Unit (FMU), the eye of the subject, and the several detection systems available. The function of the DBLS is to produce a single beam of light having the required beam divergence and having the two spectral components at 650 nm and 805 nm which are suitable for measuring the oxygen saturation of blood. The FMU, a modified Topcon Retinal Camera, projects this beam of light into the eye through the dilated pupil of the eye, collects the light reflected from the fundus of the eye, and focuses this reflected light onto a photodetector. The FMU also contains a viewing light source of adjustable intensity which can be used to observe the fundus of the subject when desired. The electrical signal from the photodetector is then sent to the Electronic System for amplification and processing. Using analog computational circuitry the Electronic System calculates the oxygen saturation from the information contained

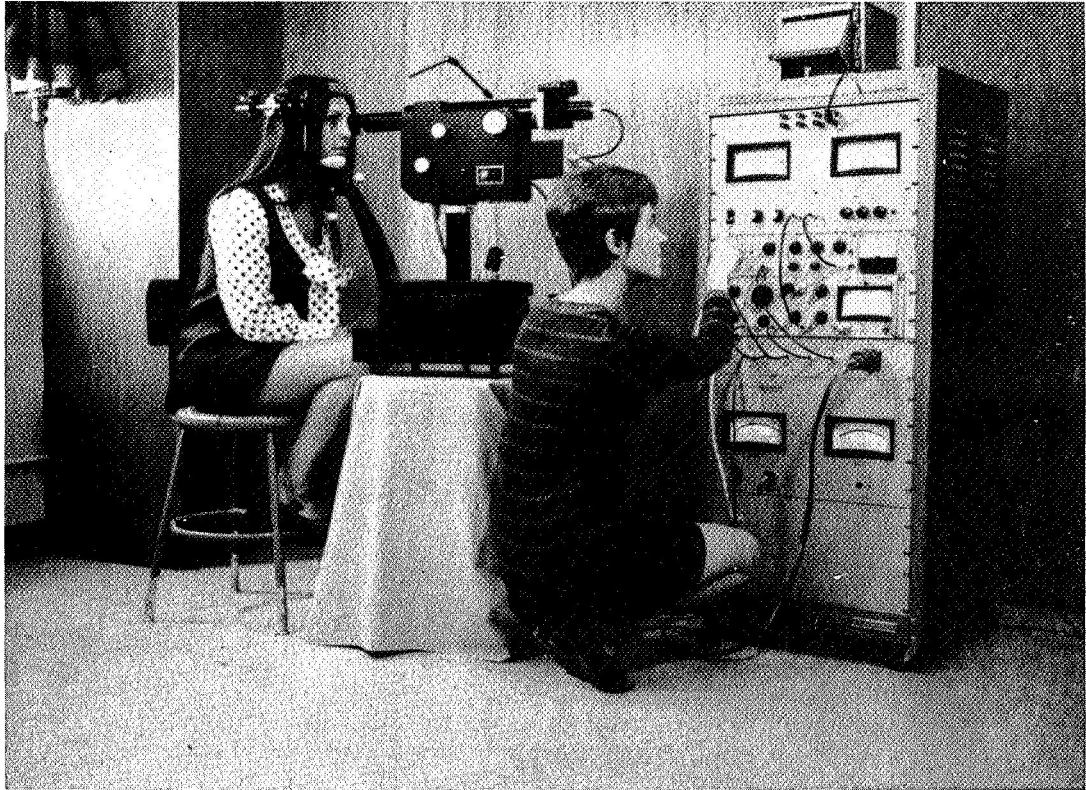
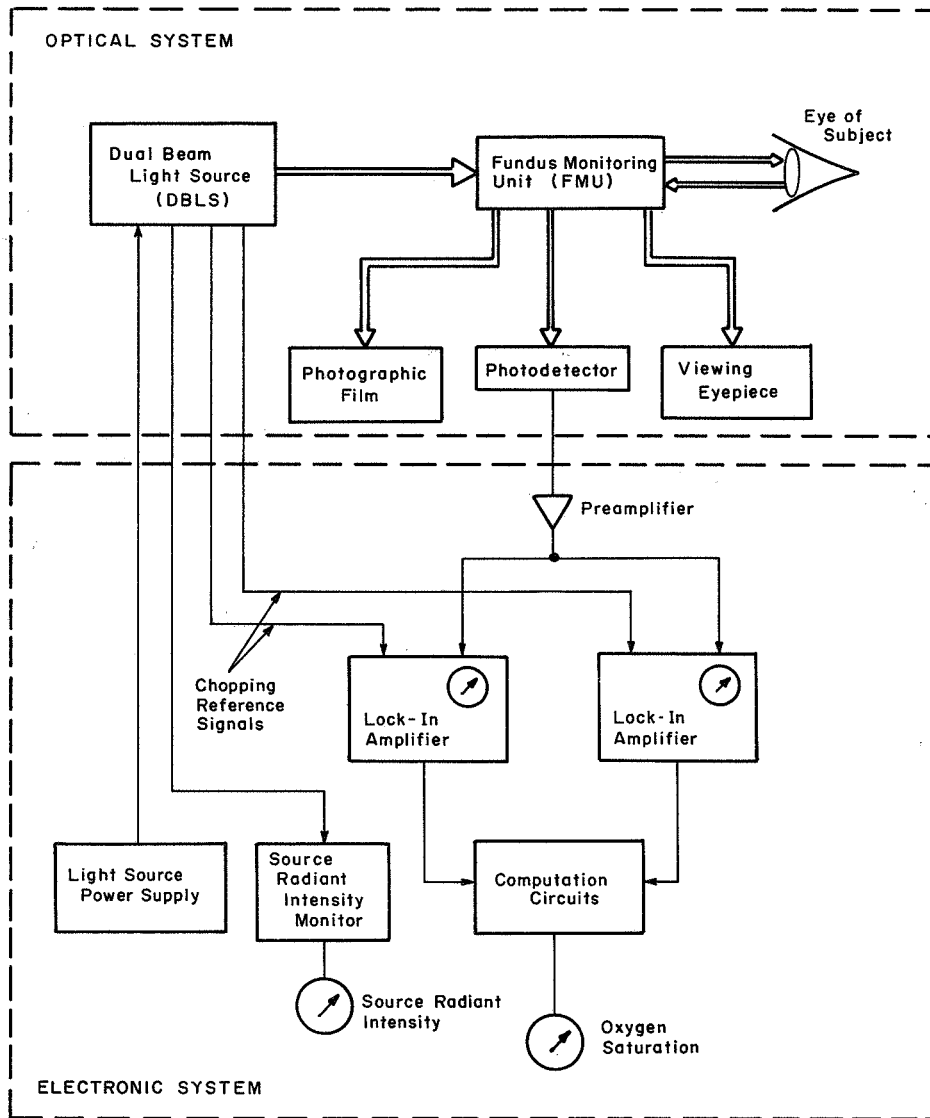


FIGURE 1.
THE EYE OXIMETER.



Notes:

== Multichromatic Light Beams

— Electrical Signal Cables

FIGURE 2.

THE MULTI-CHROMATIC EYE OXIMETER.

in the photodetector signal and displays the value of the oxygen saturation on a panel meter or on an external strip chart recorder.

3.1 The Optical System

An optical layout diagram of the DBLS is shown in Figure 3. Prior to a consideration of the optical details of the DBLS several design features should be noticed. Lenses L1 and L2 are identical, lenses L3, L4, and L5 are identical, and dichroic mirrors DM1 and DM2 are complementary coated, as shown in Figure 4. M1 and M2 are full-silvered, front surface mirrors. Each of the two light paths $Q1 \rightarrow DM1 \rightarrow M1 \rightarrow DM2 \rightarrow FB$ and $Q1 \rightarrow DM1 \rightarrow M2 \rightarrow DM2 \rightarrow FB$ is optically antisymmetrical about the intermediate image planes located at CH1 and CH2. This optical antisymmetry eliminates or reduces many of the optical aberrations which would otherwise be present. This in turn enables lenses of small f-number to be used to provide a highly compact unit with high optical efficiency. The two light paths are also optically identical to one another, which results in the same beam divergence and magnification for each light path and enables the two spectral beams to be brought into exact coincidence at the output of the DBLS.

In Figure 3, Q1 is an FCS 150-watt quartz-iodide lamp which operates at a nominal 24 volts and has a rectangular filament of nominal dimensions 2.9 mm x 5.8 mm. The FCS lamp is located at the focus of L1, an f/0.68 aspheric condensing lens which has a collection angle of 45°. DM1 is a dichroic mirror coated so as to transmit all wavelengths less than 690 nm and reflect all wavelengths greater than 750 nm. The transmission versus wavelength curves for DM1 and DM2 are shown in Figure 4. IF1 and IF2 are standard 2-inch diameter interference filters having peak transmission wavelengths of 650 nm and 805 nm, respectively. The 650-nm filter has a bandwidth at half maximum transmission of 40 nm while the 805-nm filter has a 10 nm bandwidth at half maximum. Each of these filters is easily interchangeable with any two-inch diameter 3/16-inch thick glass filter without realignment of the system. Lenses L3 and L4 are

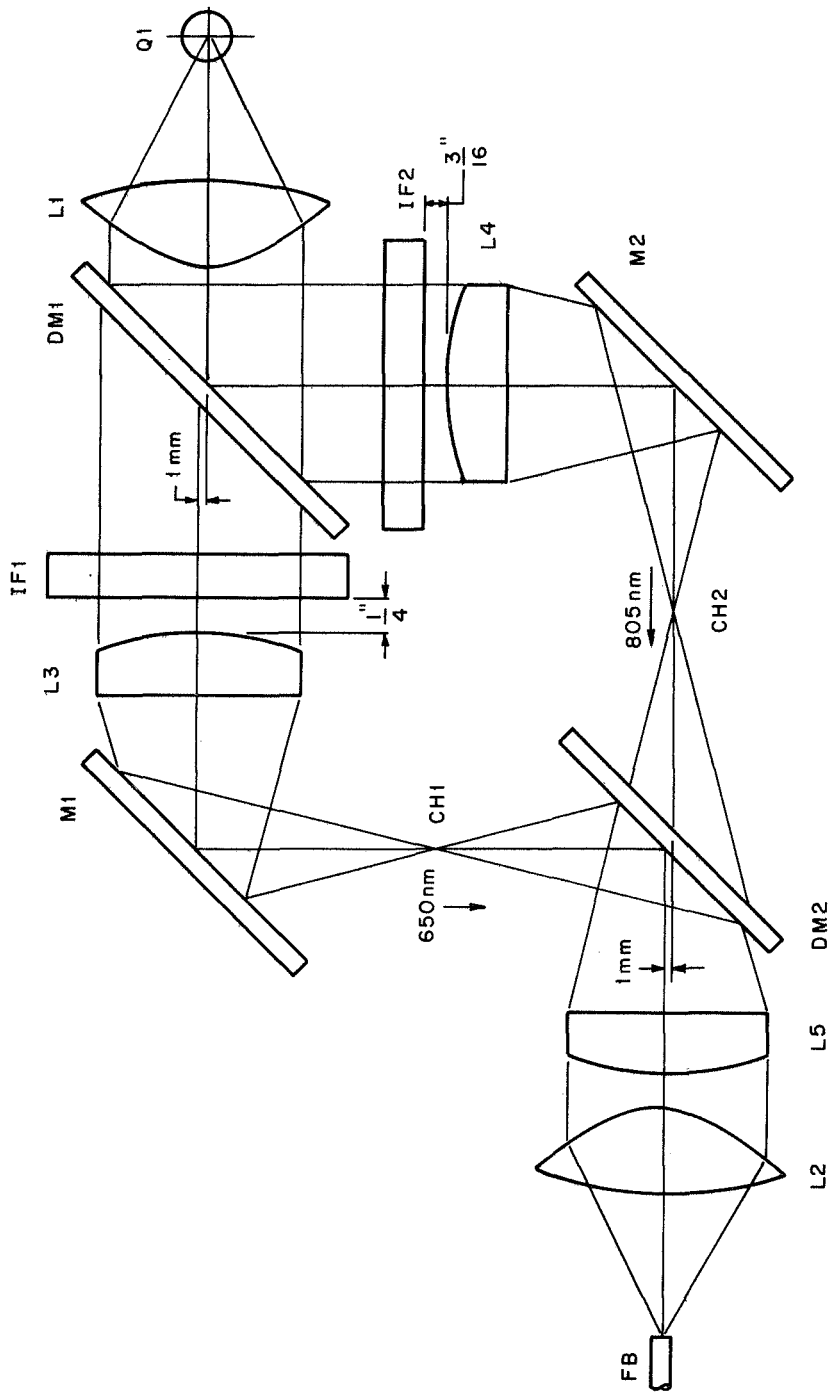


FIGURE 3.
OPTICAL LAYOUT DIAGRAM OF DBLS.

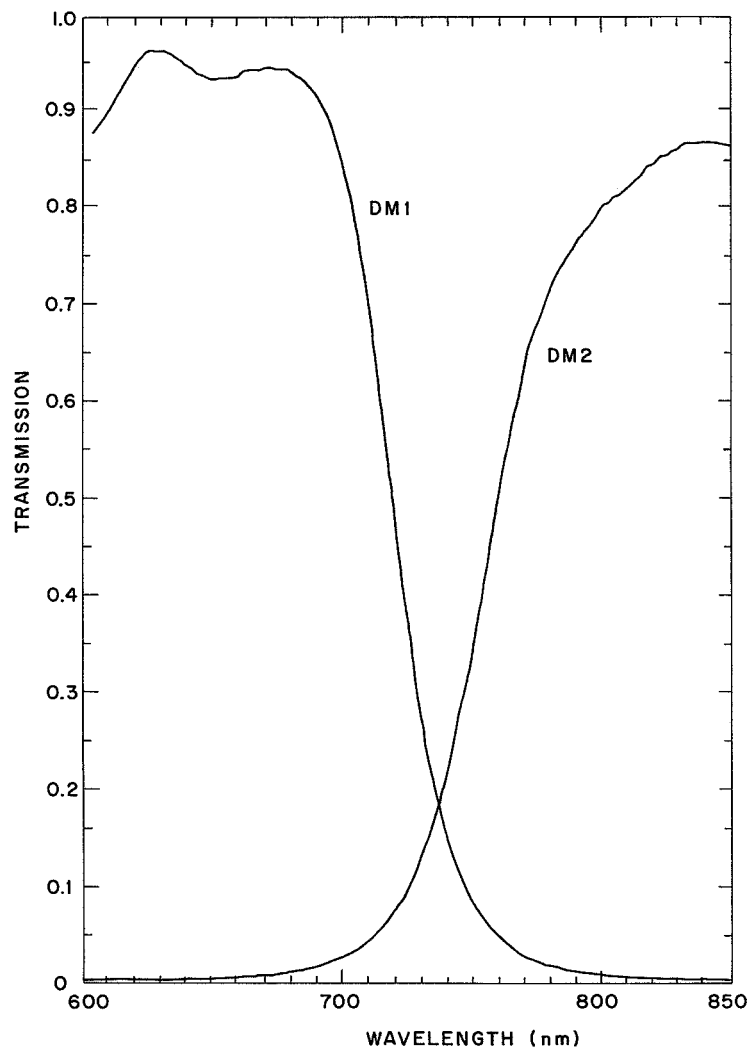


FIGURE 4.
TRANSMISSION CURVES FOR DM1 AND DM2.

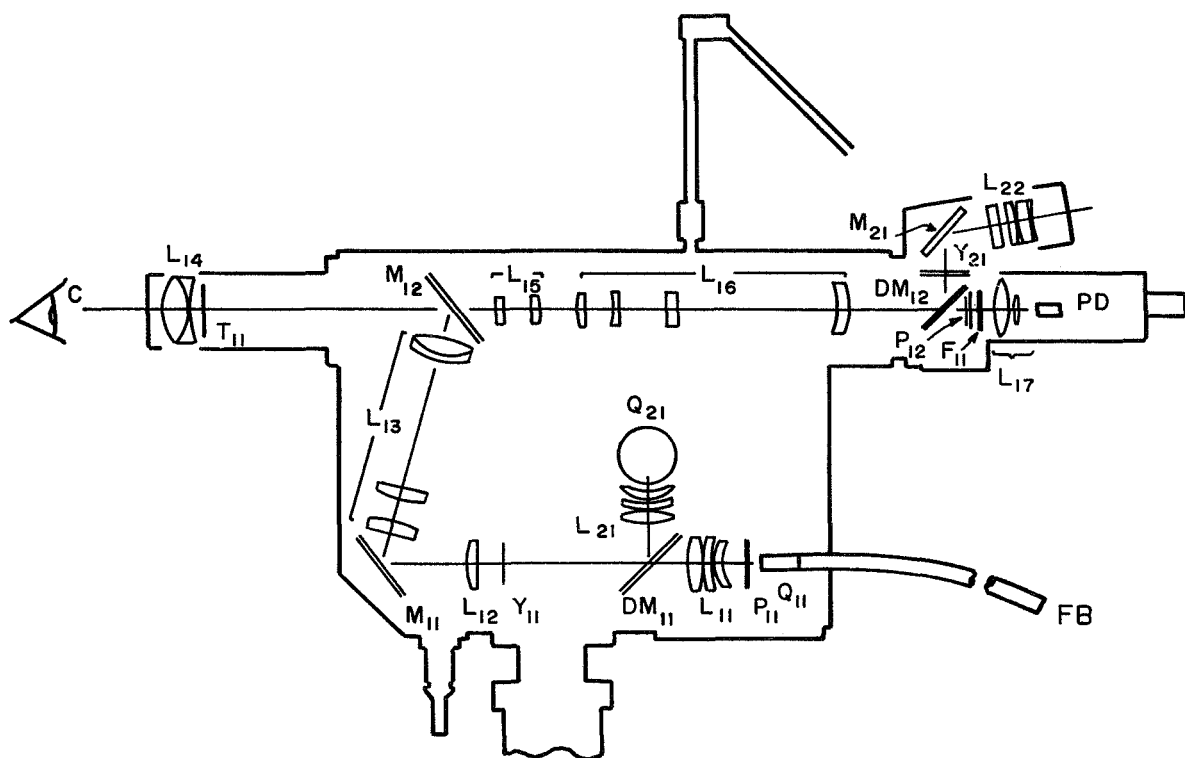


FIGURE 5.
OPTICAL DIAGRAM OF FUNDUS MONITORING UNIT.

f/2.2 achromatic doublets which serve to focus the nearly monochromatic beams of light transmitted through the interference filters in the chopping planes of the Bulova tuning fork choppers CH1 and CH2. The chopper CH1 interrupts the 650-nm beam of light 100 times per second while CH2 interrupts the 805-nm beam of light 150 times per second. Each of the choppers operates in an approximately sinusoidal mode. The front-surface full-silvered mirrors M1 and M2 serve to reflect each beam as shown. The dichroic mirror DM2 is coated so as to transmit the 805-nm beam of light and reflect the 650-nm beam and thus enables the two spectral components to be combined into a single multichromatic beam of light which is rendered parallel by lens L5, another f/2.2 achromatic doublet which is identical to lenses L3 and L4. The f/0.68 aspheric condensing lens L2, which is identical to lens L1, focuses the multichromatic beam of light onto the end of a 1/8-inch diameter incoherent fiber-optic bundle FB. This 24-inch-long fiber-optic bundle serves to transmit the multichromatic light beam from the DBLS to the Fundus Monitoring Unit.

An optical diagram of the Fundus Monitoring Unit is shown in Figure 5. The end of the fiber-optic bundle, FB, from the DBLS serves as the measuring light source Q11. The condensing lens L11 collects the light radiated by Q11 and focuses the image of the end of the fiber-optic bundle onto the iris diaphragm, Y11. The image of the bundle end is then refocused onto the front surface mirror M12 (which has a central hole in it) by lens L12, mirror M11, and lens system L13. The objective lens L14 and the cornea C of the subject reimage the end of the fiber bundle into the pupillary plane of the subject provided that the distance between the cornea and lens L14 is properly adjusted by the operator. The optics of the eye are such that imaging in the pupillary plane provides the "Maxwellian View," whereby a fixed area of the fundus is uniformly illuminated. In the Eye Oximeter the illuminated area of the fundus subtends a 28° angle, which is determined by the collection angle of the collecting lens L11.

The reflected light from the fundus, which passes through the central non-illuminated portion of the dilated pupil and is collected by the objective lens L14 of the fundus camera, is imaged at the location of the fixation target, T11. The reflected light then passes through the hole in mirror M12 and is focused on the field stop F11 after passing through the lens systems L15 and L16 and the dichroic mirror DM12. The dichroic mirror is coated so as to transmit wavelengths greater than 600 nm and reflect wavelengths less than 570 nm. The field lens system L17 serves to focus the light reflected from the fundus onto the 0.2 mm-diameter sensing area of the Hewlett-Packard HP-4204 PIN photodiode, PD. The adjustable field stop F11 enables the average oxygen saturation over a field variable from 1.5° to 28° to be measured. Due to the design of the field lens system L17 the sensing area of the photodiode which is illuminated is independent of the opening of the field stop. Specular reflections from the eye and the optical system are eliminated or reduced at the photodiode by crossed polarizing filters P11 and P12.

During visual observation of the fundus, light radiated by the incandescent viewing lamp, Q21, is collected by lens L21 and, after reflection by dichroic mirror DM11, travels to the eye through the same optical path as does the measuring light. The viewing light which is reflected from the fundus passes through the same optical path as the measuring light until it reaches the dichroic mirror DM12, where the viewing light is reflected and an image of the fundus is formed on the ground glass reticle plate Y21. The subject's fundus is observed by looking at the ground glass reticle plate through eyepiece L22 and mirror M21.

Photography of the subject's fundus is accomplished by replacing the field stop and field lens system with the original Topcon camera back or a Polaroid camera back attachment.

3.2 The Electronic System

3.2a General. A block diagram of the electronic circuitry is shown in Figure 6. This circuitry is physically located in the Fundus Monitoring Unit, the DBLS, and the relay rack. Wherever possible, commercially available modules and sub-assemblies have been used in the construction, as in the case of the phase-lock detectors. The construction is such that removal of sub-assemblies is relatively easy, facilitating servicing of the equipment.

3.2b Power Distribution. All equipment is powered from one line cord that comes out of the lower right-hand side of the relay rack. This cord should be plugged into a standard, grounded 105-125 VAC outlet. The line cord is connected via a 7.5 Amp circuit breaker (MAIN CIRCUIT BREAKER) on the front of the relay rack to a power outlet strip on the inside rear wall of the rack. This outlet strip supplies power to all of the electronic equipment in the oximeter.

3.2c FCS Lamp Power Supply and Light Monitor. The FCS lamp located in the DBLS obtains its power from a regulated supply located in the relay rack. The heart of this supply is the Electronic Research Associates, Inc., (ERA) Model LC3210 Silicon Variable DC Power Module, located on the bottom shelf of the relay rack. The Power Module is controlled from the front panel by means of a one-turn potentiometer labeled FCS FILAMENT VOLTAGE ADJ. The module is capable of delivering from 0 to 30 VDC but is limited to an upper value of 24 VDC by a resistor in parallel with the potentiometer (see Figure 7). The module is rated at 0.05% or 8 mV voltage regulation for a 0 - 100% change in load, and $\pm 0.01\%$ or 5 mV for a 20 VAC change in line voltage. Range taps are selected by a jumper wire located behind the FCS LAMP POWER SUPPLY & LIGHT MONITOR panel between the two meters. These taps do not grossly affect the output voltage, but determine the range over which the supply will be regulated within the above specifications. Normally, the FCS lamp is operated at 22.5 VDC with the regulation jumper in the 21-25 volt position. If a lamp voltage outside this range is used, the jumper must be moved to a range that includes the lamp voltage.

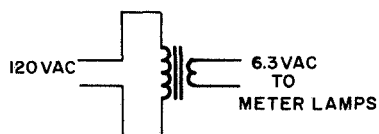
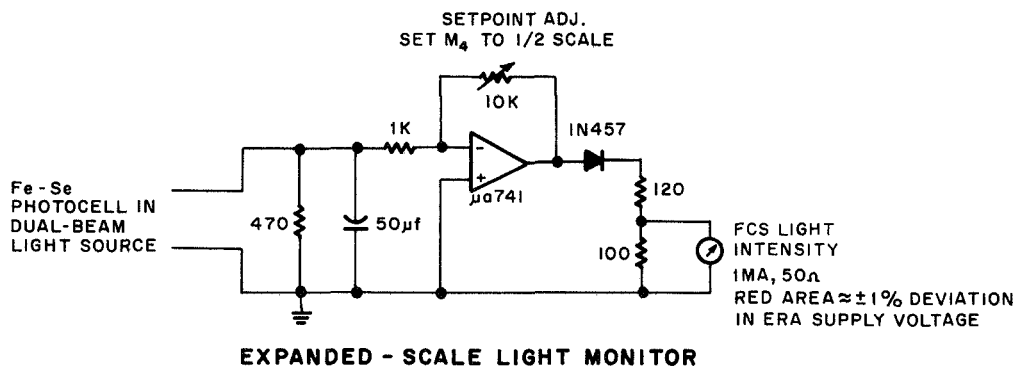
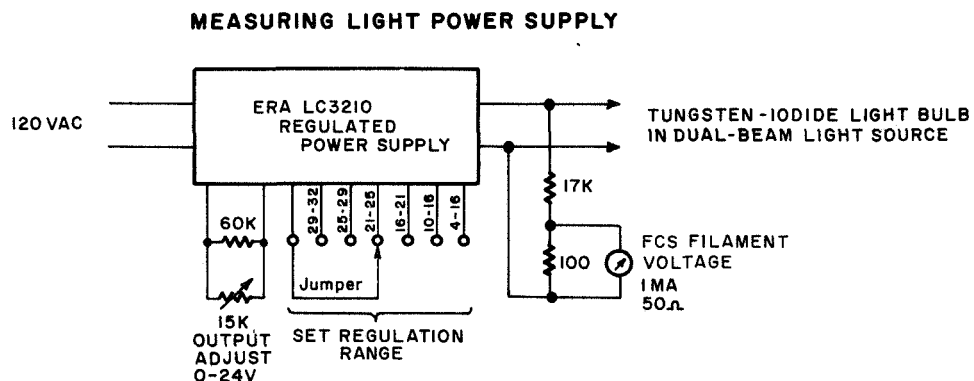


FIGURE 7.
**SCHEMATIC DIAGRAM OF FCS LAMP POWER SUPPLY
AND LIGHT MONITOR.**

The output of the FCS LAMP POWER SUPPLY is connected to the lamp via the DBLS Power Cable (terminated in 16-pin Amphenol connectors) which leaves the relay rack from a patch panel located directly above the FCS LAMP POWER SUPPLY & LIGHT MONITOR panel. See Table I for pin connections of this cable. The voltage supplied to the FCS lamp is monitored by the FCS FILAMENT VOLTAGE meter M3.

AC line power is supplied to the ERA power supply module through an illuminated ON/OFF switch on the front panel. This switch also controls the ventilation fan (105-125 VAC) in the DBLS and the pilot lamps that illuminate the two meters on the panel. The power for these lamps is supplied by a small 6.3 VAC transformer mounted on the rear of the front panel.

The ERA supply module is internally protected against short circuits and overload, and recovers automatically. Further information on this module can be found in the manufacturer's data sheets supplied with the instrument.

The light output of the FCS lamp is monitored by the Light Monitor circuit. In the DBLS an Iron-Selenium photocell mounted behind a window of heat-shielding glass receives light from the FCS lamp and generates a voltage proportional to its intensity. This voltage is fed to the Light Monitor Circuit mounted on the back of the FCS LIGHT MONITOR meter via the DBLS POWER cable (see Table I). The photocell is terminated in a resistor selected so that the sensitivity of the photocell is minimally affected by changes of temperature in the DBLS. The remainder of the circuit amplifies the signal from the photocell (gain is adjusted by the front-panel screwdriver adjustment SETPOINT ADJ.) and fed to meter M4 through a semiconductor diode and resistor network. The diode has the effect of greatly compressing the lower end of the meter scale so that at mid-scale the meter is extremely sensitive to small changes in the light intensity of the FCS lamp. The circuit is designed so that the red range at the center of the FCS LIGHT MONITOR meter represents a change in FCS light intensity equivalent to that of changing the FCS lamp voltage approximately $\pm 1\%$.

TABLE I

SCHEDULE OF CABLE CONNECTIONS

DBLS POWER (16-PIN AMPHENOL)

<u>PIN #</u>	<u>Connection</u>
A	-15 VDC
B	120 VAC
C	120 VAC
I	Fe-Se Photocell Black (Neg.) Lead
J	Ref. Signal from 100 Hz Chopper
K	Ref. Signal from 150 Hz Chopper
L	+ 15 VDC
M	Ground (OVDC)
N	- FCS Lamp Supply Voltage
P	+ FCS Lamp Supply Voltage

FUNDUS MONITOR POWER (5-PIN AMPHENOL)

<u>PIN #</u>	<u>Connection</u>
A	+ 24 VDC
B	Ground (OVDC)
H	120 VAC
E	120 VAC
D	- 24 VDC

FUNDUS MONITOR POWER (4-PIN SHIELDED)

<u>PIN #</u>	<u>Connection</u>
1	+ 24 VDC
2	- 24 VDC
3	120 VAC
4	120 VAC
Shield	Ground (OVDC)

Power for the FCS Light Monitor is obtained from the ± 15 VDC supply in the COMPUTATION CIRCUITRY MODULE. The reading of the FCS LIGHT MONITOR meter will drift somewhat when the Oximeter is first turned on, due to temperature changes within the DBLS and due to thermal changes associated with the filament of the FCS lamp, but after 5 to 10 minutes the meter should remain well within the red band assuming that it is properly adjusted and that the FCS lamp has not deteriorated with age. Dirt on the heat-shielding glass, FCS lamp, or photocell could be responsible for any changes in the reading of the Light Monitor, so this should be checked if the reading of the Light Monitor is found to deviate from normal.

3.2d Light Choppers. There are two American Time Products (Bulova) Light Choppers in the Dual Beam Light Source. Each Chopper consists of a tuning fork to which vanes are attached. An electronic driver circuit initiates and maintains the mechanical motion of the fork at its natural frequency. An adjustment on each driver circuit can be used to change the amplitude of oscillation of the fork. This adjustment has been set for maximum amplitude and should not be changed.

The chopper that modulates the 650 nm beam has a natural frequency of 100 Hz. The chopper for the 805 nm beam has a natural frequency of 150 Hz. Each chopper circuit generates a reference waveform of frequency equal to that of its tuning fork. These reference signals travel through the DBLS POWER cable (see Table I) to the Phase-Lock Detectors, where they provide phase reference for each detector.

Power for the chopper drivers is obtained from the ± 15 VDC supply in the COMPUTATION CIRCUITRY MODULE via the DBLS POWER cable. The choppers are self-starting and should reach full amplitude within approximately 40 seconds. If a chopper does not start, ascertain that no wires are touching the tuning fork, as this will prevent the fork from oscillating.

3.2e Photodetector. A Hewlett-Packard HP-4204 PIN Photodiode is used as the photodetector in the camera back of the FMU. The detailed characteristics of this photodiode are given in the manufacturer's data sheets supplied with the oximeter.

As shown in Figure 8, the photodiode is biased in the reverse direction to a level of 1.4 VDC by a small mercury cell (Burgess HG312) in the camera back. This cell is held in a Plexiglass clamp and can be removed for replacement by a firm push on the edge of the cell. Note that the positive terminal of the cell is connected to a red wire. The cell should last almost as long as its normal shelf life, as its minimum possible load resistance is 22 megohms. Routine replacement of the mercury cell is recommended at one-year intervals to forestall unexpected failure of the photodiode circuit.

The photodiode circuit responds in a linear fashion to changes in the intensity of light impinging on the photodiode aperture over the range of intensities encountered in the oximeter. Because of the high output impedance of the photodetector circuit, the cable from this circuit to the PAR 112 Preamplifier must be as short as possible. Do not substitute a longer coaxial cable for this connection.

3.2f Photodetector Preamplifier. The AC output of the photodiode circuit is fed to a Princeton Applied Research (PAR) 112 Preamplifier mounted on the back of the FMU. This preamplifier has a voltage gain of 100, and special low-noise characteristics as described in the manufacturer's instruction manual supplied with the instrument. At 100 Hz and 150 Hz, the noise figure of the preamplifier is less than 2.0 db. Input impedance of the Preamplifier is 100 megohms shunted by 30 pf.

The \pm 24 VDC power for the Preamplifier is obtained from an octal socket on the back of the PAR 121 Phase-Lock Detector (mounted in the relay rack). This power leaves the relay rack at the Interconnection panel through the FUNDUS MONITOR POWER cable.

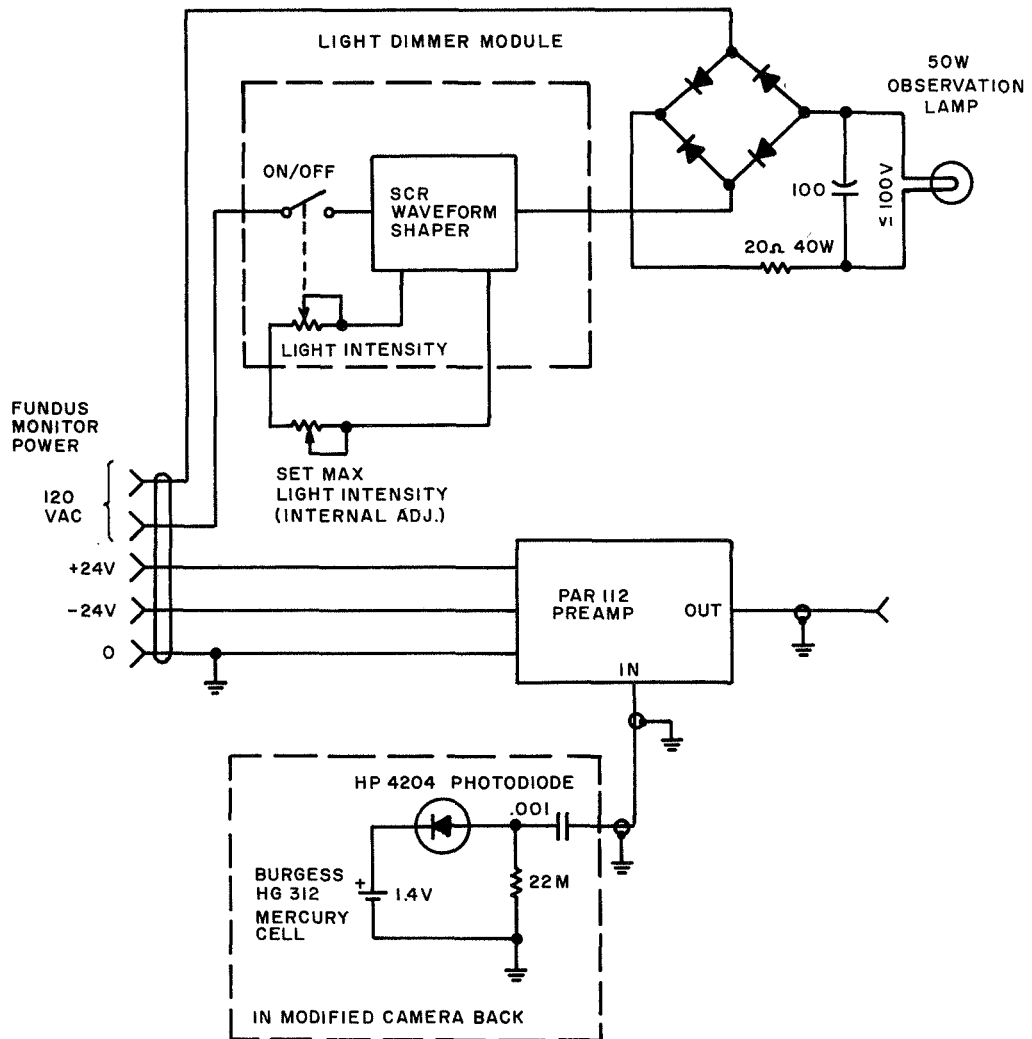


FIGURE 8.
SCHEMATIC DIAGRAM OF
ELECTRONICS IN FUNDUS MONITOR.

The output impedance of the Preamplifier is 1000 ohms, which is sufficiently low compared to the input impedance of the phase-lock detectors (10 megohms shunted by 30 pf) that there is no diminution of signal level due to a voltage drop across the output impedance.

3.2g Observation Light Power Supply. The power supply for the observation lamp in the FMU consists of a variable silicon-controlled rectifier circuit that shapes the AC line waveform and a full-wave bridge rectifier and filter (see Figure 8). All of this circuitry is contained in the FMU.

The SCR waveform shaper (a modified "light-dimmer" module) is a compact means of changing the voltage to the observation light without dissipating the unused power as heat. It is controlled by a combination push-on-push-off switch and potentiometer mounted on the side of the FMU. When the potentiometer is fully counterclockwise, no voltage is applied to the observation lamp. The voltage applied to the lamp when the potentiometer is fully clockwise is determined by the setting of a 10-turn "trimpot" mounted inside the FMU beneath the fiberglass circuit card holding the filter resistors. The 105-125 VAC for the Observation Light Power Supply is supplied via the FUNDUS MONITOR POWER cable.

Servicing of the Observation Light is accomplished without removing the side cover of the FMU. The cylindrical protrusion on the side of the FMU case that has only two knobs can be pulled out. This cylinder contains the Observation Lamp and its socket. This lamp should burn out infrequently because of its low operating voltage.

3.2h Interconnecting Panel. The Interconnecting Panel is located immediately above the FCS LAMP POWER SUPPLY & LIGHT MONITOR panel on the relay rack, as shown in Figure 9.

The three leftmost BNC connectors on the Interconnecting Panel are connected together so that the output cable from the Photodetector Preamplifier may be fed simultaneously to the inputs of both Phase-Lock Detectors. The other two BNC

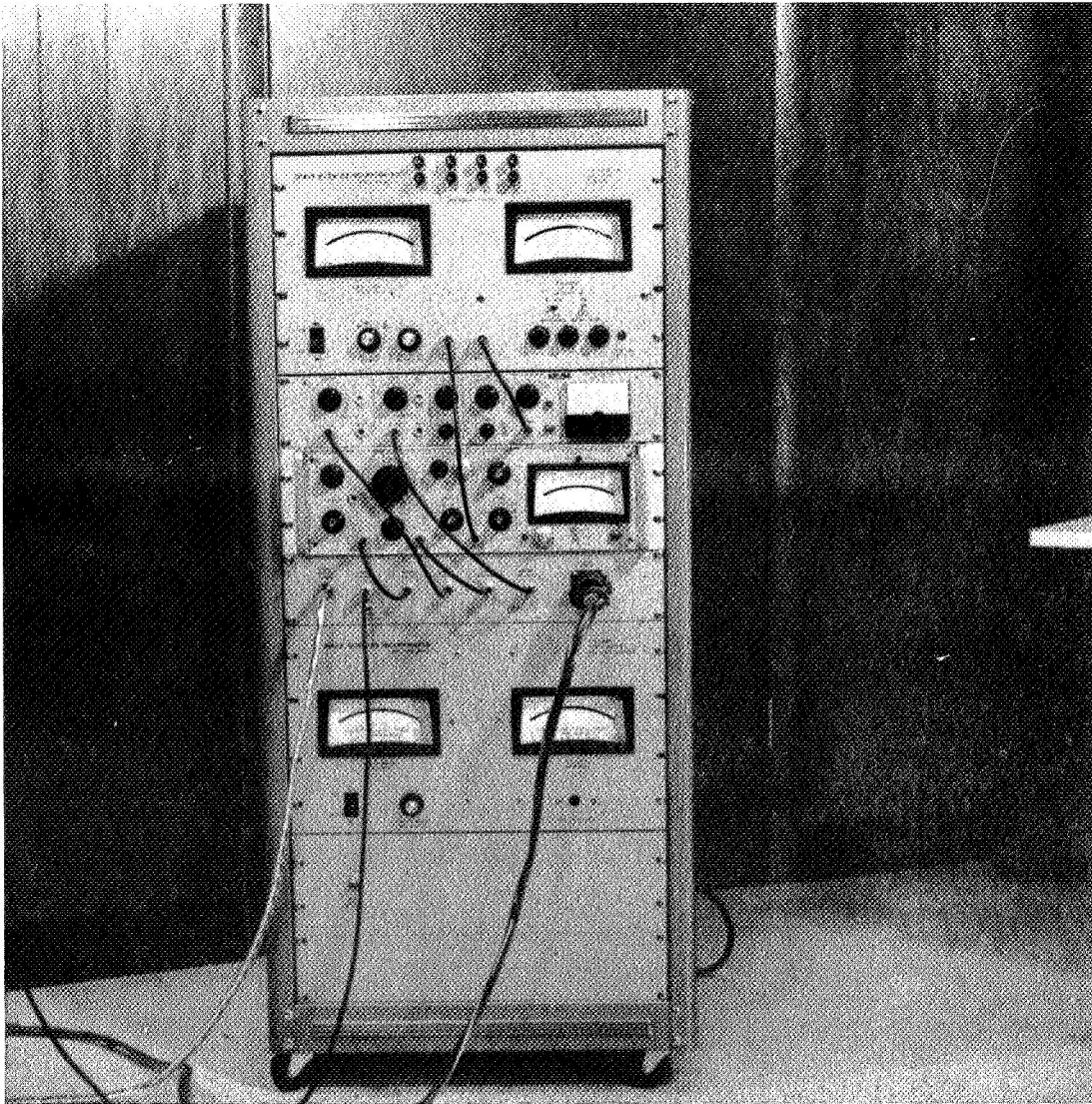


FIGURE 9.
THE RELAY RACK.

connectors are connected behind the panel to the two leads from the DBLS POWER cable carrying reference waveforms from the Light Choppers (see 3.2d). On the front of the panel, they are connected by means of shielded cables to the reference inputs of the two Phase-Lock Detectors. Table I describes the connections of the two Amphenol sockets on the Interconnecting Panel.

A toggle switch below the PAR 112 OUTPUT connector places a resistor in parallel with the output of the Preamplifier, reducing its output voltage by approximately 90% if desired. It is necessary to use this SIGNAL ATTENUATOR switch to prevent overloading of the Phase-Lock Detectors under certain conditions described in section 4.3.

3.2i Phase-Lock Detectors. The AC signal from the Photodetector Preamplifier is fed simultaneously to the PAR 120 and PAR 121 Phase-Lock Detectors via the connections on the PATCH PANEL. The PAR 120 is tuned (internally) to a frequency of 150 Hz and has applied to it the reference waveform from the 150 Hz Light Chopper. The PAR 121 is tuned to 100 Hz by a front-panel control and uses the 100 Hz chopper waveform as a reference. When properly adjusted, each Phase-Lock Detector will amplify, rectify, and filter the portion of the signal from the Photodetector that is in phase with and at the same frequency as, the Light Chopper that provides its reference voltage. Thus the output of the PAR 120 is a DC voltage proportional to the intensity of chopped light of 805 nm reflected from the fundus, and the output of the PAR 121 is a DC voltage proportional to the intensity of chopped light of 650 nm reflected from the fundus. Any signals from stray light that has not passed through the Light Choppers, as well as unwanted electrical pickup such as 60 and 120 Hz hum, will be rejected by the frequency- and phase-selectivity of the Phase-Lock Detectors.

The MONITOR output voltage of the Phase-Lock Detectors can be ± 10 VDC. However, except during some of the calibration procedures, the output voltage will always be positive. The MONITOR jacks on the Phase-Lock Detectors are connected via shielded cables to the two BNC connectors on the

COMPUTATION CIRCUITRY MODULE in the relay rack.

Detailed information on the characteristics, servicing, and maintenance of the Phase-Lock Detectors will be found in the manufacturer's instruction manuals supplied with the instrument.

3.2j Computation Circuitry Module. The function of the COMPUTATION CIRCUITRY MODULE (CCM) is to divide the signal from the PAR 120 by the signal from the PAR 121 and to calculate, in a convenient form, the function $S_R = -a(Z - Z_0) + b$ where $Z = I_R(805)/I_R(650)$ is the ratio of the signals from the Phase-Lock Detectors and a , Z_0 , and b are constants selected by front-panel controls.

The division is performed by a GPS Model DIV 502 analog divider module mounted behind the front panel on a sub-chassis. The divider has a rated accuracy of 0.5% of full-scale (see manufacturer's data sheets supplied with the Eye Oximeter). This accuracy is realized only if the divider inputs are nearly ideal voltage sources. For this reason LM 302 integrated-circuit voltage followers are used to condition the input signals to the divider. A DIFFERENTIAL BALANCE ADJ. dual-potentiometer is connected between the inputs of the voltage followers and the MONITOR outputs of the Phase-Lock Detectors as shown in Figure 10. This potentiometer allows adjustment of the relative intensities of the outputs, so that when the model eye is in place or a subject is breathing 100% oxygen, the outputs can be adjusted to the ratio 8/10. This is an arbitrary but convenient ratio that prevents the REFLECTED INTENSITY meter from reading off-scale during decreases in oxygen saturation and provides a point of standardization for the calibration procedure, as described later in this section.

The divider has two outputs. One is +10 volts times the ratio of the input voltages, the other is -10 volts times the ratio of input voltages. The positive output is connected to the 10 IR/RED recorder jack and is read by the REFLECTED INTENSITY meter when it is switched to the 10 IR/RED position. The negative output is connected to the remainder of the computation circuitry. Each of the outputs can vary from -10 to +10 volts and has an impedance of 0.01 ohm. The

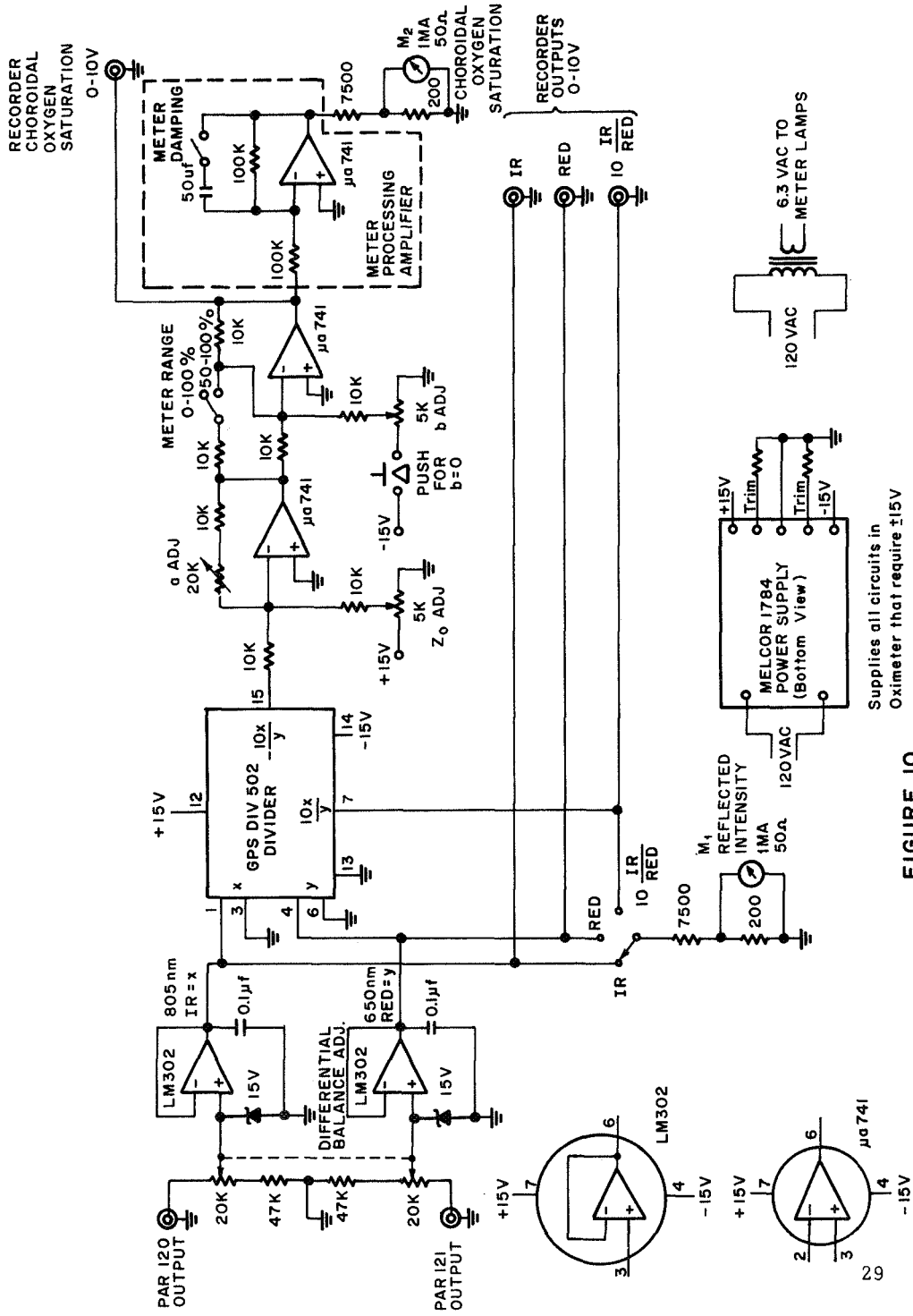


FIGURE 10. SCHEMATIC DIAGRAM OF COMPUTATION CIRCUITRY MODULE.

REFLECTED INTENSITY meter, when switched to the IR position, reads the voltage at the numerator (805 nm) input of the divider. In the RED position, the voltage at the denominator input (650 nm) is indicated by the meter. Since the accuracy of the divider is dependent on maintaining its inputs at as high a level as possible, the Phase-Lock Detectors should always be adjusted (see Section 4.3) so that they have a maximum on-scale meter deflection.

The REFLECTED INTENSITY meter can be used as a double-check to ascertain that the divider is being provided with optimum signal levels and that there are no malfunctioning components up to that point. The same three circuit points that are read by the REFLECTED INTENSITY meter are also connected to the three leftmost recorder jacks on the COMPUTATION CIRCUITRY MODULE panel. These recorder outputs have an impedance of less than one ohm and provide a 0 to +10 VDC signal.

The computation is performed on the output of the divider by two $\mu A741$ integrated-circuit operational amplifiers and associated circuitry. These amplifiers, as well as the two voltage followers, are mounted on a circuit card next to the divider.

The first amplifier has a voltage gain of from -1.0 to -3.0 depending on the setting of the front-panel control, a ADJ. The two inputs to this amplifier, the negative output of the divider and the adjustable voltage from the $Z_{\circ} ADJ.$ potentiometer, are of opposite polarity. Thus, when the output of the divider is -8.0 volts, as it is during the calibration procedure for the Oximeter, the $Z_{\circ} ADJ.$ control can be varied to adjust the output of the first operational amplifier to zero, as described in Section 4.3. Oxygen saturation will normally decrease from this condition, thereby decreasing the output from the PAR 121 and increasing the absolute value of the ratio. Since the ratio feeding the first operational amplifier is negative, this will result in an increasing, positive signal at its output.

The output of the first operational amplifier is one of the inputs to the second operational amplifier, which has a voltage gain of -1.0 or -2.0, depending on the position of the METER RANGE switch of the COMPUTATION CIRCUITRY MODULE. The other input is the negative voltage from the "b ADJ." potentiometer. This second input can be set to zero by depressing the "PUSH FOR b= 0" switch during the calibration procedure. This permits one to read the output of the first amplifier on the CHOROIDAL OXYGEN SATURATION meter so that it may be set to zero. After this step in the calibration procedure, the "b ADJ." potentiometer is adjusted to produce a reading of 97 % on the CHOROIDAL OXYGEN SATURATION meter. Since the output of the first amplifier will increase in a positive direction for decreases in saturation, this will produce a decrease from the 97% reading, due to the negative gain of the second operational amplifier. The output of the second operational amplifier is connected to the recorder jack labelled CHOROIDAL OXYGEN SATURATION and to the Meter Processing Amplifier.

The Meter Processing Amplifier has a DC voltage gain of -1.0, but can be used to increase the damping of the CHOROIDAL OXYGEN SATURATION meter (but not the recorder jack) beyond that provided by the Phase-Lock Detectors by throwing the METER DAMPING switch to 'ON'. As supplied to the user, the time constant of this circuit is approximately 5 seconds. The time constant may be changed if desired by changing the capacitor on the Meter Processing Amplifier circuit card mounted on the back of the CHOROIDAL OXYGEN SATURATION METER. The value of capacitor required may be calculated from the equation

$$C = 10 T$$

where T is the desired time constant in seconds and C is the capacitance in microfarads.

The Melcor 1784 Power Supply mounted in the COMPUTATION CIRCUITRY MODULE provides ± 15 VDC regulated to better than 0.1% under load variation

and 0.05% under line variation to the circuitry in the COMPUTATION CIRCUITRY MODULE as well as to circuitry in other parts of the Oximeter, as previously noted. A transformer mounted on the rear side of the COMPUTATION CIRCUITRY MODULE panel provides 6.3 VAC for the pilot lamps of the two meters.

For further information on the various modules in the COMPUTATION CIRCUITRY MODULE, refer to the manufacturers' data sheets supplied with the Oximeter. In case the COMPUTATION CIRCUITRY MODULE does not operate properly after shipment, ascertain that the various modules are firmly plugged into their sockets.

4. OPERATION OF THE INSTRUMENT

4.1 Preliminary Calibration and Adjustment of the Electronics

The following section describes the technique for calibrating, testing, and adjusting the Lock-In Amplifiers prior to making a measurement of choroidal oxygen saturation using the Eye Oximeter. The calibration procedure described in Section 4.1.1 may be by-passed if the operator is confident that the Lock-In Amplifiers are operating properly and if neither the GAIN ADJ. control on the PAR 120 nor the ADJ. control on the PAR 121 have been tampered with since the last time the Lock-In Amplifiers were calibrated. It is recommended, however, that the calibration of the Lock-In Amplifiers be checked every three months.

4.1.1 Calibration of the Lock-In Amplifiers. The following procedure is provided to facilitate calibration and checking of the PAR Lock-In Amplifiers. This procedure presupposes no knowledge of the instrument on the part of the operator. Should any difficulty be encountered in carrying out these checks, contact the PAR factory or one of the PAR authorized representatives listed in the back of the PAR instruction manual.

Calibrating the PAR 120 Lock-In Amplifier

Procedure:

1. Disconnect all BNC cables from the front panel of the PAR 120.
2. Turn the POWER switch to ON. The pilot lamp should come on provided that the line cord is plugged into a "hot" outlet.
3. Wait five minutes before proceeding to allow the instrument to warm up.
4. Set the front panel controls as follows:

SENSITIVITY	50 mv.
MODE	CAL. 1 mv
PHASE, top control	0°
PHASE, bottom control	0°

TIME CONSTANT	30 ms.
METER/MONITOR KNOB	OUT x 10

5. Adjust the ZERO knob so that the meter reads 0.
6. Turn the METER/MONITOR knob to SIG.
7. Connect a BNC coaxial cable from the Reference IN/OUT jack of the PAR 120 to the signal INPUT jack of the PAR 120.
8. Set the sensitivity switch to 1 mv. The meter should indicate between 45% and 85% of full scale.
9. Adjust the signal FREQ. TRIM control for maximum meter deflection.
10. Set the SENSITIVITY Control to "50 mv."
11. Set the METER/MONITOR switch to OUT X1 .
12. Adjust the bottom PHASE control for maximum meter deflection to the left of center.
13. Set the GAIN ADJ. control to give a full scale meter deflection.
14. Remove the BNC coaxial cable from the Reference IN/OUT jack and the Signal INPUT jack.

This completes the initial calibration and testing of the PAR 120 Lock-In Amplifier.

Calibrating the PAR 121 Lock-In Amplifier

Procedure:

1. Disconnect all BNC cables from the front panel of the PAR 121.
2. Turn the POWER switch to ON. The pilot light should come on provided that the line cord is plugged into a "hot" outlet.
3. Wait five minutes before proceeding to allow the instrument to warm up.
4. Set the front panel control as follows:

SENSITIVITY	20 mv.
SIGNAL Q	10
FREQUENCY Hz dial	10
Frequency MULTIPLIER	10.0

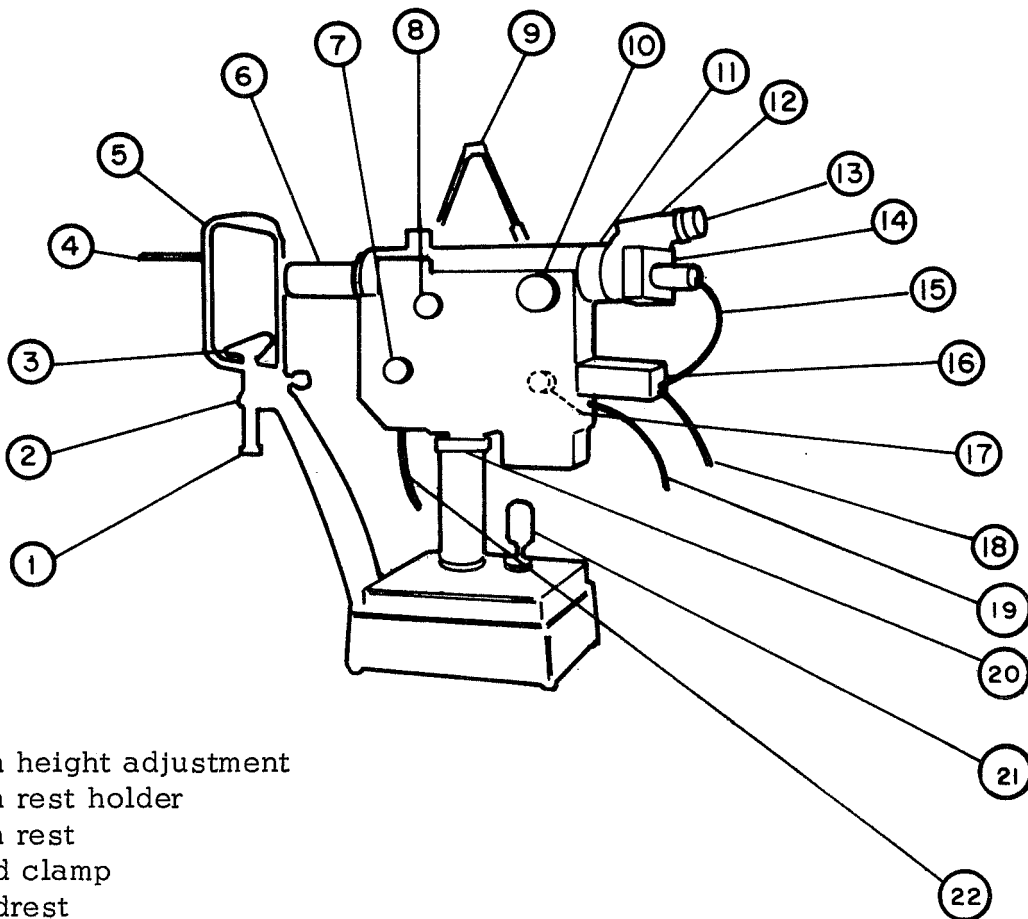
PHASE control, left knob	0°
PHASE control, right knob	0°
TIME CONSTANT	30 ms.; 6 db/octave
MODE	CAL. 10 mv.
METER/MONITOR switch	SIG.
ZERO SUPPRESS toggle switch	Center Position
ZERO SUPPRESS control	Any position
REF. ATTEN. switch	1
REF. ATTEN. VERNIER	fully clockwise

5. Connect a BNC coaxial cable from the REF. IN/OUT of the PAR 121 to the SIG. IN jack of the PAR 121.
6. Adjust the FREQ. TRIM control for maximum deflection (about 50% of full scale to the right of center).
7. Set the SENSITIVITY control to 10 mv.
8. Set the ADJ. control with a screwdriver to give a full scale meter deflection.
9. Remove the BNC coaxial cable from the REF. IN/OUT jack and the SIG. IN jack.

This completes the initial calibration and testing of the PAR 121 Lock-In Amplifier.

4.1.2 Preliminary Adjustment of the Electronics. Referring to Figures 9 and 11, connect BNC coaxial cables between the various jacks as shown. Notice that the jacks are labeled in such a way so as to facilitate connecting the cables between the proper jacks.

The following procedure enables the proper signal, reference, and phase adjustments of the Lock-In Amplifiers to be made using the signals obtained from the electronics located in the DBLS.



Key:

- | | |
|--|---|
| <ul style="list-style-type: none"> 1. Chin height adjustment 2. Chin rest holder 3. Chin rest 4. Head clamp 5. Headrest 6. Objective lens barrel 7. Illumination diaphragm knob 8. Diopter compensation knob 9. External fixation target 10. Focusing control 11. Attachment ring for Polaroid camera back assembly 12. Eyepiece assembly 13. Eyepiece lens 14. Field stop, field lens, and photodetector housing 15. Coaxial cable from photodetector housing to INPUT of photodetector preamplifier 16. Photodetector preamplifier | <ul style="list-style-type: none"> 17. Viewing light control (on opposite side) 18. Coaxial cable from OUTPUT of photodetector preamplifier to PAR 112 OUTPUT on Interconnecting Panel 19. Fiber optic bundle from DBLS 20. Height adjustment 21. Joy stick 22. Cable from FMU to FUNDUS MONITOR POWER on Interconnecting Panel |
|--|---|

FIGURE II.
FUNDUS MONITORING UNIT.

Procedure:

1. Set the SENSITIVITY control of each Lock-In Amplifier to its maximum value.
2. Throw the SIGNAL ATTENUATOR switch located just below the PAR 112 OUTPUT jack on the Interconnecting Panel to ON .
3. Turn on the power switches in the FCS LAMP POWER SUPPLY AND LIGHT MONITOR panel and wait five minutes for the equipment to warm up.
4. Adjust the FCS FILAMENT VOLTAGE ADJ. control until the FCS LIGHT MONITOR meter reads mid-scale. The FCS FILAMENT VOLTAGE meter should then read between 22 and 23 volts for "normal" operation. If it does not and the "normal" operating mode is desired, adjust the FCS FILAMENT VOLTAGE ADJ. control until the FCS FILAMENT VOLTAGE meter reads 22.5 v. Using a small screwdriver adjust the SETPOINT ADJ control to give a mid-scale reading on the FCS LIGHT MONITOR .
6. A low intensity beam of red light should be noticed coming out of the objective lens of the Fundus Monitoring Unit (FMU) at this time (provided that the viewing lamp of the FMU is off). Insert the Model Eye supplied with the FMU into the chin rest holder (2) of the FMU, shown in Figure 11. Using the Joy Stick (21) and Height Adjustment (20) controls, adjust the FMU and the Model Eye so that a sharp image is formed slightly above the center of the pupil of the Model Eye.

Adjusting the PAR 120 Lock-In Amplifier

1. Set the front panel controls as follows:

SENSITIVITY	50 mv.
MODE	SEL. EXT.
TIME CONSTANT	30 msec.
METER/MONITOR switch	REF.

2. With a screwdriver adjust the Reference FREQ. TRIM control (not the Signal FREQ. TRIM control) to give a maximum meter deflection.

3. With a screwdriver adjust the Reference LEVEL ADJ. control to give a half-scale meter deflection. (The PAR meters are zero-center devices. Half-scale means mid-way between "0" and either the right or left end-points.)
4. Set the METER/MONITOR switch to SIG.
5. Set the SENSITIVITY control to give the highest ~~on-scale~~ reading.
6. Adjust the Signal FREQ. TRIM control to give a maximum meter deflection. Readjust the SENSITIVITY control if necessary.
7. Set the METER/MONITOR switch to OUT X1.
8. Adjust the bottom PHASE control to give a maximum positive meter deflection. Readjust the SENSITIVITY control if necessary. If the meter deflection will not go through a maximum as the bottom PHASE control is rotated over its allowable range then set the upper PHASE control to one of its other three positions so that a maximum deflection to the right is reached as the bottom PHASE control is rotated through its range.
9. Set the TIME CONSTANT switch to 1 sec.

Adjusting the PAR 121 Lock-In Amplifier.

1. Set the front panel controls as follows:

SENSITIVITY	500 mv
SIGNAL Q	10
FREQUENCY Hz	10.0
MULTIPLIER	10
PHASE, left control	180 ^o
PHASE, right control	0
TIME CONSTANT	30 msec.
ZERO SUPPRESS toggle switch	Center
MODE	SEL. EXT.
METER/MONITOR switch	Ref.

The other front panel controls may be set to any value.

2. Adjust the REF. ATTEN. switch to give a meter deflection of approximately half-scale.
3. Adjust the FREQUENCY Hz dial to maximize the meter deflection.
4. Adjust the REF. ATTEN. and the REF. ATTEN. VERNIER to give a meter deflection of exactly half-scale.
5. Set the METER/MONITOR switch to SIG. and adjust the FREQ. TRIM control to give a maximum meter deflection. Readjust the SENSITIVITY control if necessary.
6. Set the METER/MONITOR switch to OUT X1 and set the right PHASE control to give a maximum positive meter deflection. Readjust the SENSITIVITY control if necessary. If the meter deflection will not go through a maximum as the right PHASE control is rotated over its allowable range then set the left PHASE control to one of its other three positions so that a maximum deflection to the right is reached as the right PHASE control is rotated through its range.
7. Set the TIME CONSTANT switch to 1 sec.

This completes the preliminary electronic adjustments on the Eye Oximeter. If everything has been adjusted properly as described above the meter on the PAR 120 should read 6 ± 1 mv with the SENSITIVITY control set to 10 mv and the meter on the PAR 121 should read 13 ± 1 mv with the SENSITIVITY control set to 20 mv.

4.2 Observation of the Fundus

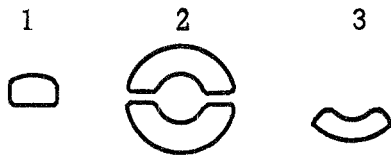
The following section describes a method for adjusting the FUNDUS MONITORING UNIT to enable the observer to satisfactorily view the fundus of the subject prior to making a measurement of choroidal oxygen saturation. Although a satisfactory measurement of choroidal oxygen saturation can easily be made without previously viewing the fundus it is generally advisable to obtain a satisfactory viewed image prior to the measurement. This enables the operator to be confident of the fundus area which is being measured and provides him with a means of

looking for any unusual retinal pathologies which might affect the readings of oxygen saturation which will be obtained.

Referring to Figure 11, have the subject sit comfortably with his chin in the rest (3) and his forehead snug against the headrest (5). The chin height adjustment (1) should be rotated until the head clamp (4) lies just above the ears. The pressure pads on the head clamp (4) should be adjusted so that the front pads lie just behind the temples and the rear pads lie just above the posterior portion of the ears. The pads should be screwed in so that they contact the head firmly but not uncomfortably.

Set the index of the diopter compensation knob (8) to engraving "+ 8/-10" which is the normal range for the emmetropic or non-emmetropic eye. The figures indicate the vertex power range of the subject.

Set the index of the illumination diaphragm knob (7) to engraving "1". The



relationship between illumination diaphragm and numbers is shown in Figure 12. Although the instrument is designed to be used with diaphragm 1 the other diaphragms may be useful for special situations.

FIGURE 12
ILLUMINATION DIAPHRAGMS

Switch on the viewing light by pushing the knob (17). The intensity of the viewing light can be adjusted by rotating the knob of this control.

The eyepiece (13) should be adjusted to the operator's eye by rotating the eyepiece lens (13) until the horizontal and vertical cross-hairs are in sharp

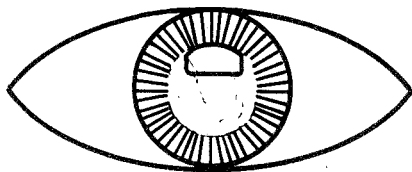


FIGURE 13
IRIS DIAPHRAGM IMAGE

focus. In order to align the iris diaphragm image with the patient's pupil, adjust the elevating wheel (20) and joy stick (21) until the iris diaphragm image is observed within the pupil of the patient's eye, as in Figure 13, when the pupil is observed directly

from the side of the Fundus Monitoring Unit (and not through the eyepiece lens). The fine alignment of the Fundus Monitoring Unit is accomplished by looking through the eyepiece lens (13) and adjusting the joy stick (21) and elevating wheel (20) slightly until all reflection is eliminated from the field of view. The retinal image should be seen more or less distinctly at this time.

Focus the viewed retinal image by revolving the focusing control (10). Do not make further adjustments with the joy stick (21). Focusing is completed if the retinal image and the horizontal/vertical cross-hairs of the eyepiece are seen distinctly at the same time. If difficulty is obtained in seeing the retinal vessels the focusing knob (10) can be rotated until the diagonal cross-hairs are in sharp focus. This set of cross-hairs, which should be used as a fixation target if the macular oxygen saturation is to be determined, lies near an image plane of the subject's retina. This design feature results in the retinal image and the diagonal cross-hairs being in focus at nearly the same setting of the focusing control (10).

If focusing cannot be undertaken in the preceding way, a diopter compensation lens must be placed in the light path. Revolve the diopter compensation knob (8) and set the index to engraving "-10/-22" in the case of a strong myope, or to "+ 8/+ 25" in the case of a strong hyperope, and re-focus as described above. (For viewing the ocular anterior, the index can be set to "⊙".) In order to fix the direction of the patient's line of vision, have the patient gaze at the intersection of the diagonal cross-hairs with the measured eye or at the external fixation target (9) with the free eye. If there is need to change the direction of the line of vision, readjust the joy stick (21) and elevation adjustment (20) as described above.

This completes the adjustment of the Fundus Monitoring Unit to the subject's eye and should result in a satisfactory viewed image of the fundus as well as a suitable electronic signal being fed to PAR 112 Preamplifier (16).

4.3 Final Adjustment of the Electronics and Calibration of the Eye Oximeter

Following the proper alignment of the Fundus Monitoring Unit with the subject's eye as described in the preceding section, the final adjustments of the system are made as follows with the subject breathing normal room air.

The SENSITIVITY controls on both the PAR 120 and the PAR 121 should be set so that each of the output meters reads between 50 and 100% of full scale. Should the signal from the PAR 112 Preamplifier be so large that an on-scale reading cannot be obtained on the PAR 120 then the SIGNAL ATTENUATOR switch located just below the PAR 112 OUTPUT jack in the Interconnecting Panel should be thrown to ON. Normally however, this switch should be in the OFF position.

With the REFLECTED INTENSITY knob on the COMPUTATION CIRCUITRY MODULE set to $10 \times IR/RED$, the DIFFERENTIAL BALANCE ADJ. should be set so that the reflected intensity meter reads 8.0. A red index mark is provided on the meter face at this value.

The METER RANGE switch for the CHOROÏDAL OXYGEN SATURATION Meter should be set to either 50 - 100% or 0 - 100% as desired. The METER DAMPING switch should be set to the desired position. For static measurements of oxygen saturation it is recommended that this switch be set to ON. The method of calibration and adjustment described is independent of the setting of these switches.

The "PUSH FOR $b = 0$ " switch should be depressed and the Z_0 ADJ. control set for a zero reading on the CHOROÏDAL OXYGEN SATURATION meter. The "PUSH FOR $b = 0$ " switch should be released and the "b ADJ." control set to give a meter reading of either 97% or (preferably) the directly measured value of the arterial oxygen saturation of the subject. To determine the proper setting for the "a ADJ." control the subject should breathe an artificial 9% O_2 - 91% N_2 gas mixture. After the signal has reached its new steady state value the "a ADJ." control should be set to give a meter reading of either 60% or (preferably) the measured value of

arterial oxygen saturation of the subject under these new steady state conditions. The settings of the "Z₀ ADJ.", "a ADJ.", and "b ADJ." controls for the subject used should then be recorded. Resetting Z₀, a, and b to these values will permit the Eye Oximeter to read the correct value of Choroidal Oxygen Saturation for the same subject without the necessity for repeating the calibration procedure.

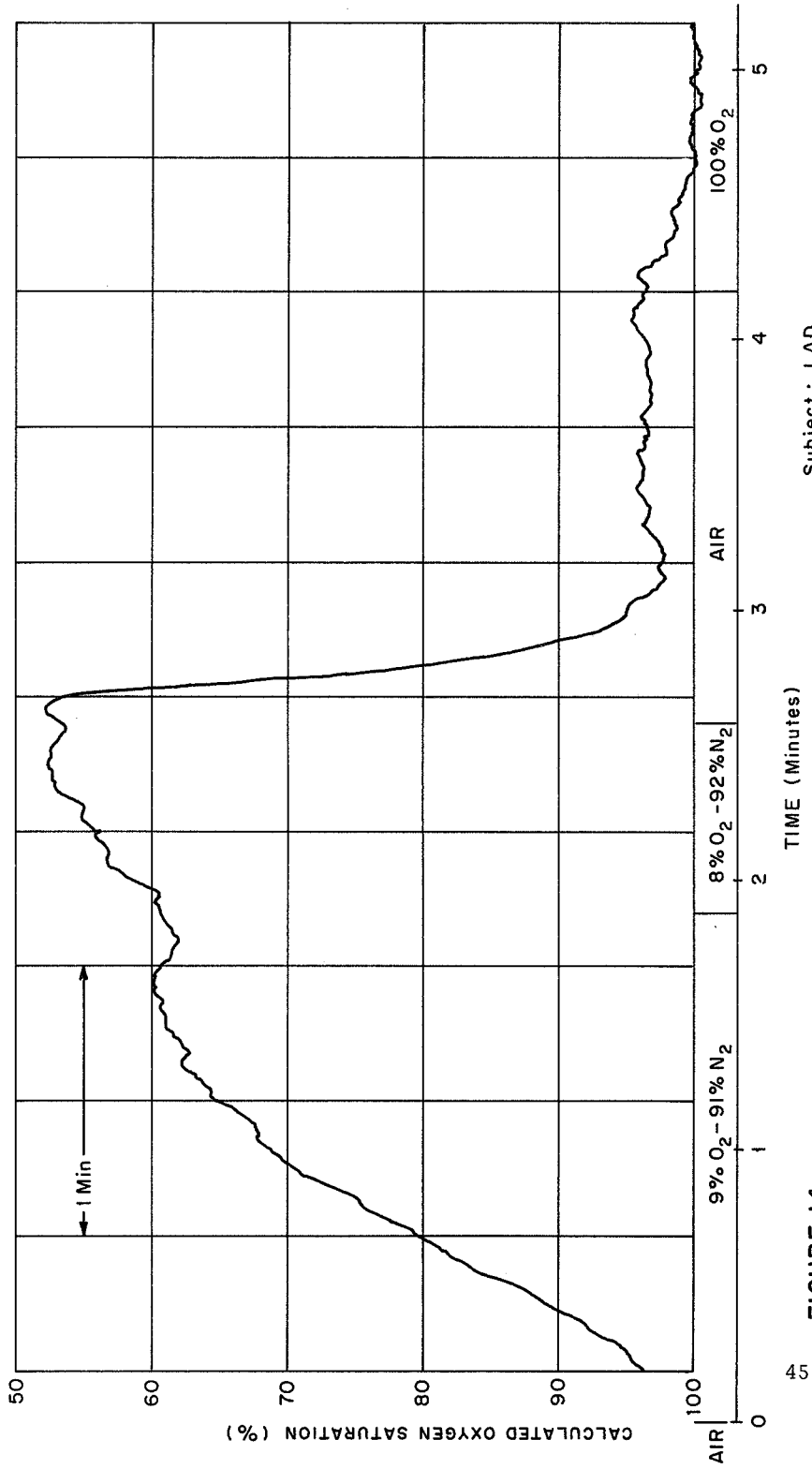
This completes the adjustment of the Eye Oximeter. The CHOROIDAL OXYGEN SATURATION meter should read the oxygen saturation to within 1% at all values between 50 and 100% provided that the measurement is truly a reflectance measurement with the oxygen saturation being given by an equation of the form $S = a \left\{ \left[\frac{I_R(805)}{I_R(650)} \right] - Z_0 \right\} + b$, where I_R(805) is the infrared (IR) reflected intensity from the fundus and I_R(650) is the red reflected intensity of the fundus. If it should turn out that the measurement is not truly a reflectance measurement as discussed above the scale on the CHOROIDAL OXYGEN SATURATION meter will not read correctly and one of the techniques discussed previously in Section 2 would have to be applied to refine the reading.

Kinetic changes of I_R(650), I_R(805), $10 \times \frac{I_R(805)}{I_R(650)}$, and Choroidal Oxygen Saturation can be measured by connecting a recorder to the appropriately labeled jack located at the top of the COMPUTATION CIRCUITRY MODULE panel. Each jack provides a 0 - 10 volt DC signal to any standard recorder.

5. PERFORMANCE OF THE EYE OXIMETER

As a preliminary evaluation of the performance of the Eye Oximeter a series of measurements was made on several subjects. During a given experiment the subject, whose left pupil was dilated with 10% Phenylephrine Hydrochloride, would inspire either room air or an artificial $O_2 - N_2$ gas mixture through a rubber tube. Expiration occurred through the nose of the subject. The O_2 concentration in the $O_2 - N_2$ mixture was monitored by a Westinghouse Oxygen Analyzer. The choroidal oxygen saturation, S , was computed by the Eye Oximeter circuitry and recorded on a Mosely Autograf Model 680 Strip Chart Recorder. The Eye Oximeter was previously calibrated to the subject using the method described in Section 4.2. The results of a typical experiment on a trained, non-fatigued, subject are shown in Figure 14. In this experiment the subject, L.A.D., breathed room air for several minutes until a steady baseline was obtained. At the time indicated in the figure the inspired gas composition was changed abruptly to a 9% $O_2 - 91\% N_2$ mixture. This step change in inspired gas composition resulted in the choroidal oxygen saturation falling to approximately 60% as shown. After the oxygen saturation had reached its new equilibrium value the gas mixture was again changed, this time to provide an 8% $O_2 - 92\% N_2$ inspired gas mixture. This resulted in a decrease of choroidal oxygen saturation to approximately 53% as shown. After this new steady state value was reached the inspired gas mixture was abruptly changed to room air and the oxygen saturation increased to the 96-97% value previously observed. The inspired gas mixture was finally changed abruptly to 100% O_2 and the saturation further increased to nearly 100% as shown.

Several physiological or artifactual sources of noise or changes in S have been observed. Figure 15 shows clearly the correlation of S with the respiration cycle. The spacing and mean frequency of 4-5 seconds for large fluctuations agrees well with the start of inspiration and the start of expiration



Subject : LAD
 DILATED LEFT PUPIL
 Time Constant : 1 Sec

FIGURE 14.
CALCULATED OXYGEN SATURATION vs.
TIME FOR CHANGES IN BREATHING MIXTURE.

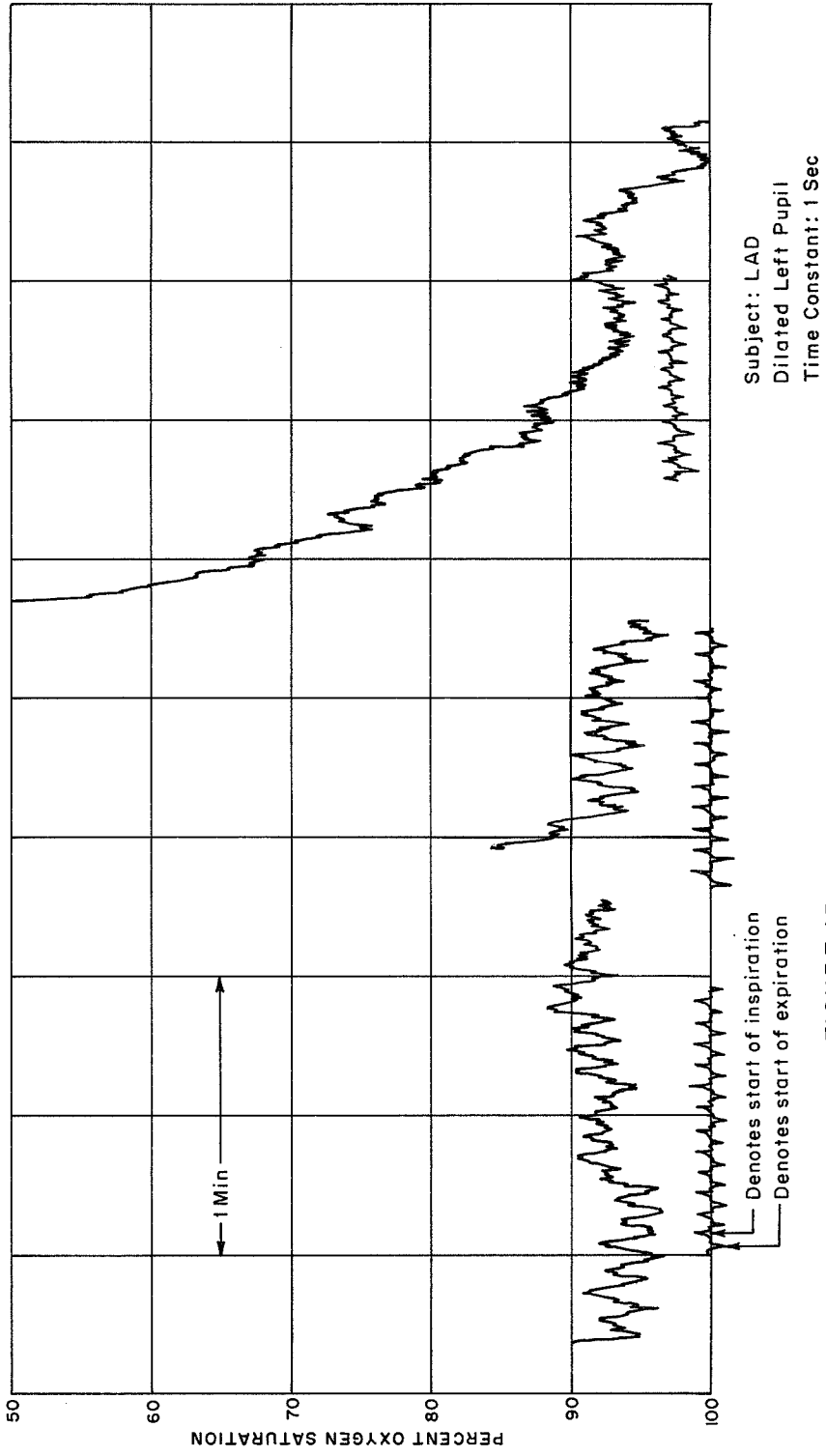


FIGURE 15.
CORRELATION OF OXYGEN SATURATION
CHANGES WITH BREATHING.

as monitored with the NASA/ERC thermistor breathing monitor. Smaller signal fluctuations, occurring at a frequency near the pulse rate of the subject, are also seen in this figure. Although these small changes could be due to pulse-to pulse variations in S, this has not yet been directly verified.

Figure 16 shows a composite drawing illustrating several artifacts which can occur in the indicated S.

Figure 17 shows the result of another experiment using the same subject, L.A.D. The experimental conditions were similar to those used to obtain the data previously shown in Figure 14. In the present case, however, the subject was fatigued and his pupil was not fully dilated. This resulted in the significant increase in noise level apparent in Figure 17 as compared to that evident in Figure 14. The tracing shown in the current figure clearly shows changes in S due to respiration and head and eye movements. Pulsatile variations may also be present.

Figure 18 shows the results of a similar experiment using a subject, R.A.L. who though moderately trained was very fatigued. Although the envelope of the curve shows the usual shape found in this type of experiment, the presence of numerous blink signals and head or eye motion artifacts considerably obscures the signal.

Figure 19 shows the tracing obtained when a plastic model eye was used in place of the real eye of a human subject.

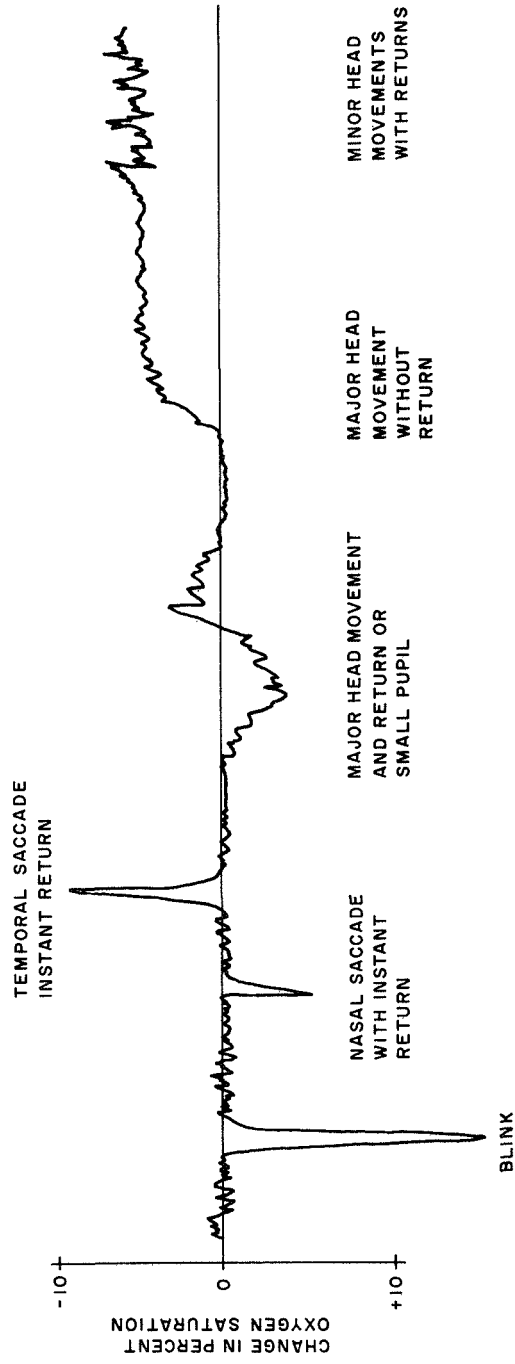
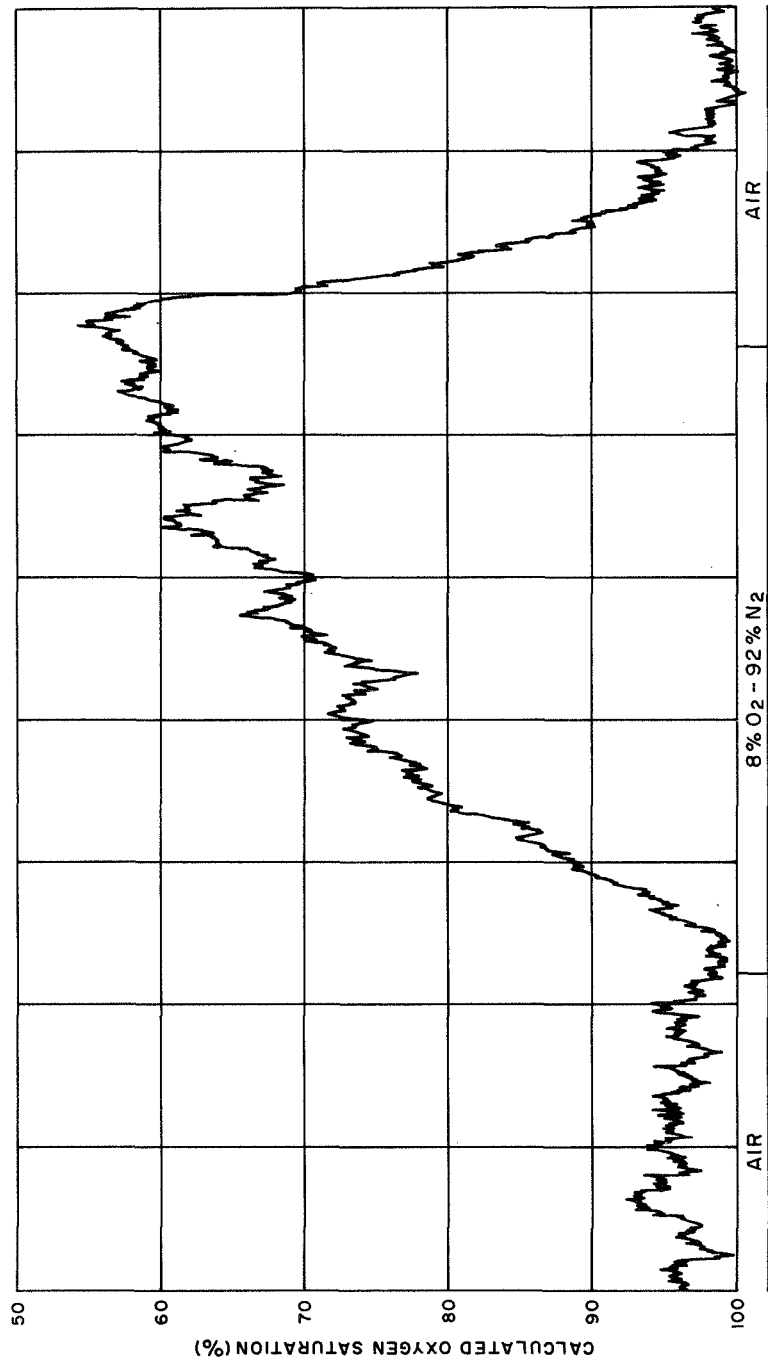


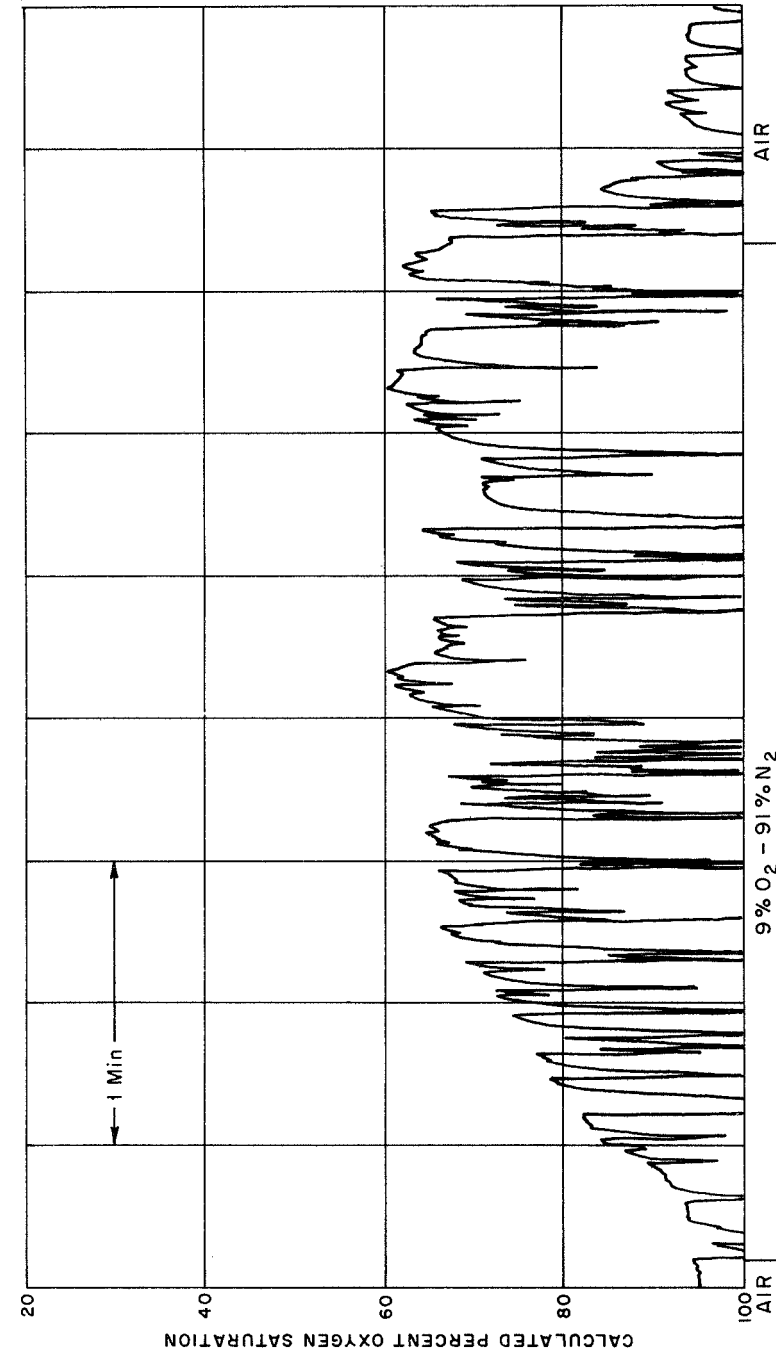
FIGURE 16.
ARTIFACTS AND SPURIOUS RESPONSES.



Subject: LAD
 PARTIALLY DILATED LEFT PUPIL
 TIME CONSTANT: 1 Sec

FIGURE 17.

COMPUTED OXYGEN SATURATION vs. TIME FOR A TRAINED FATIGUED SUBJECT
 DURING CHANGES IN BREATHING MIXTURE.



Subject: RAL
 DILATED LEFT PUPIL
 TIME CONSTANT: 1 Sec

FIGURE 18.
OXYGEN SATURATION vs. BREATHING MIXTURE
FOR A FATIGUED SUBJECT.

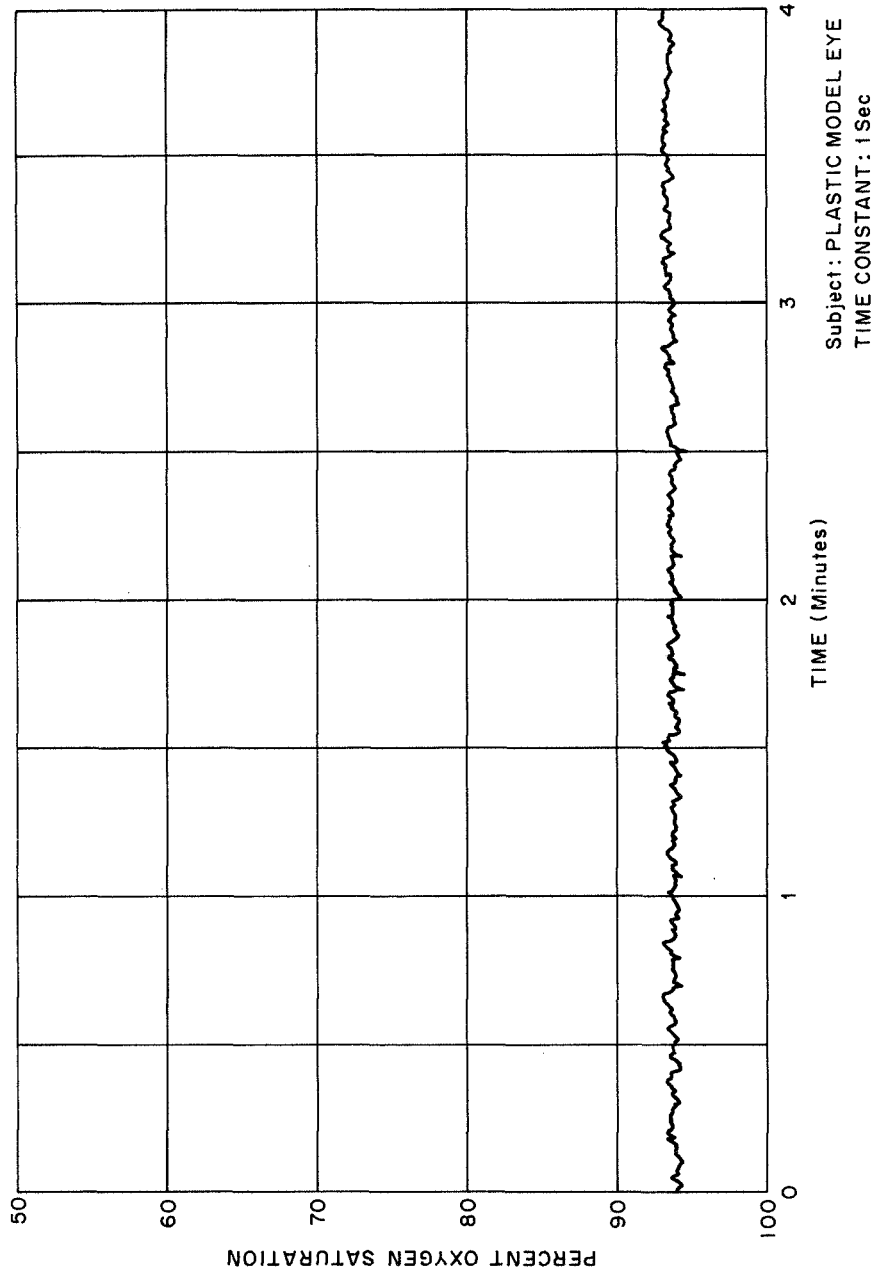


FIGURE 19.
STABILITY OF THE EYE OXIMETER.

REFERENCES

1. Broadfoot, K.D., Gloster, J., and Greaves, D.P.: Brit. J. Ophthal. 45: 161, 1961.
2. Gloster, J. and Greaves, D.P.: Exp. Eye Res. 3: 327-333, 1964.
3. Gloster, J. and Greaves, D.P.: Brit. J. Ophthal. 48: 260-275, 1964.
4. Guyton, A.C.: Textbook of Medical Physiology , W.B. Saunders Co. 1966, p. 397.
5. NASA CR-1205 (III): Compendium of Human Responses to the Aerospace Environment, (10-48) - (10-53), 1968.
6. Polanyi, M.L. and Hehir, R.M.: Rev. of Sci. Inst. 31: 401-403, 1960.
7. Millikan, G.A.: Rev. Sci. Inst. 13: 434, 1942.
8. Tait, G.R., Sekelj, P. and D'Ombrian, G.L.: IEEE Trans. on Bio-Medical Engineering, BME-13: 200-206, 1966.
9. Kay, R.H. and Coxon, R.J.: J. of Sci. Instr. 34: 233-236, 1957.
10. Adler, F.H.: Physiology of the Eye . C.V. Mosby and Co., 1965.

APPENDIX A
THEORY OF EYE OXIMETRY

This section presents the results of a first order theoretical calculation which shows that the oxygen saturation, S_R , of choroidal blood can be determined if the reflectance of two monochromatic beams of light from the choroid can be measured. In particular, a first order theoretical calculation based on a simple model of the choroid gives the result that

$$S_R = a \left[\frac{I_R(805)}{I_R(650)} \right] + b$$

where $I_R(805)$ and $I_R(650)$ are the measured reflected intensities from the choroid of light of wavelength 805 and 650 nm, respectively, and a and b are constants which depend upon the incident intensity of the light and the known molecular absorption coefficients of hemoglobin (Hb) and oxyhemoglobin (HbO_2).

A.1 Optical Properties of the Eye

Figure A-1 shows a horizontal cross section of a normal eye. The indices of refraction, n , of the refracting components of the eye are shown along with the path followed by a monochromatic ray of light of intensity $I_O(\lambda)$ and wavelength λ which reflects from the choroid and emerges from the eye with an intensity $I_R(\lambda)$. Since 1) the optically refracting parts of the eye are transparent in the visible and near infrared so that no dispersion in this region of the spectrum occurs, and 2) the amount of light which is reflected from each of the ocular interfaces is both small and independent of wavelength, it follows that $I_R(\lambda)/I_O(\lambda)$ is independent of λ and is only dependent upon the reflective properties of the choroid.

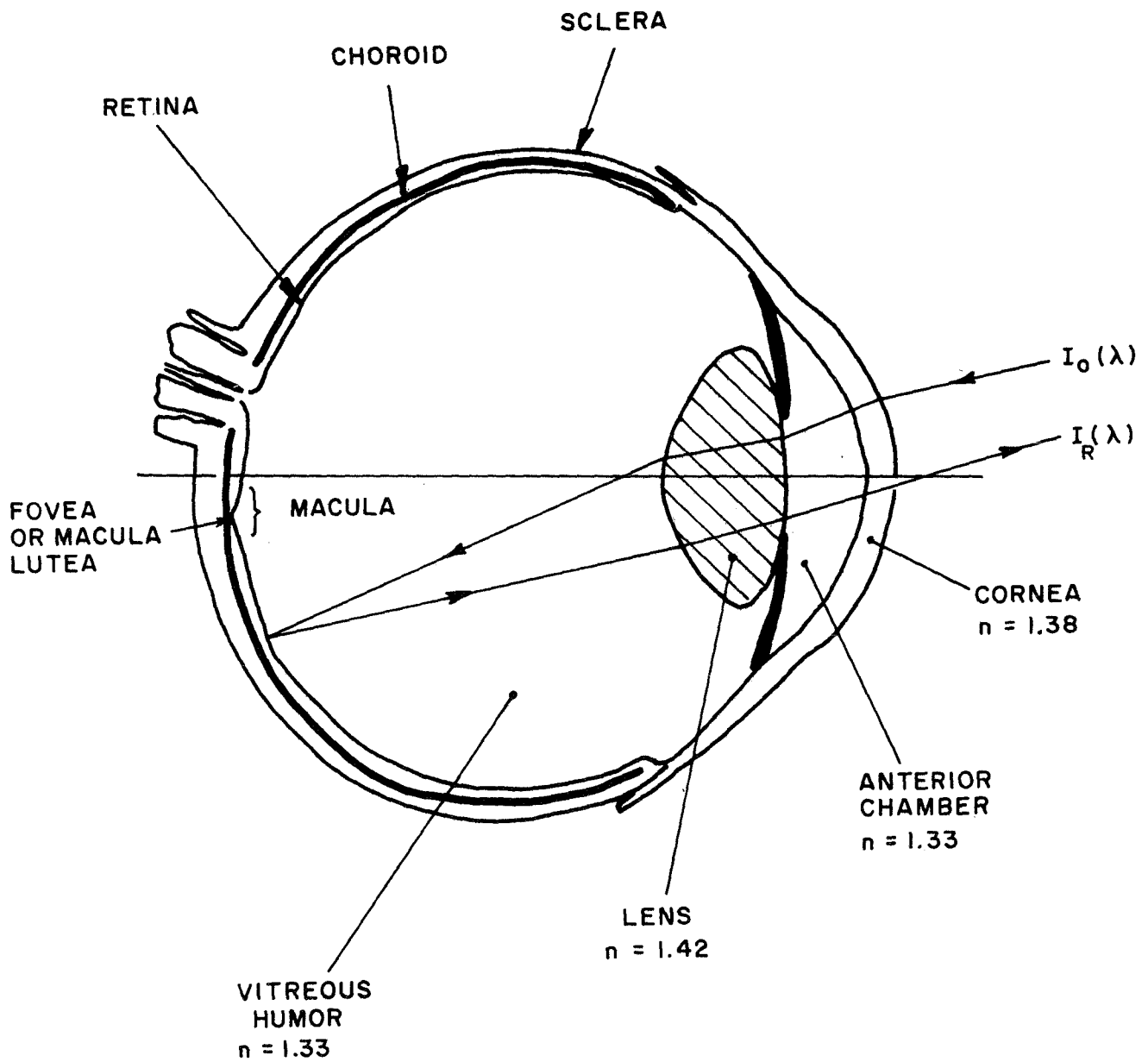


FIGURE A-1.
THE HUMAN EYE.

A.2 The Reflection of Light From the Choroid

The area of the choroid which is to be observed for its reflective properties is the posterior pole or macula which is relatively free of retinal blood vessels and allows a good view of the choroidal vasculature. The sclera, lying immediately behind the choroid, has a very small reflection coefficient at the wavelengths being used by the Eye Oximeter. Due to the large blood-to-tissue ratio of the choroid and the large optical absorption of the sclera a convenient mathematical model of the choroid can be constructed. For the purposes of theoretical analysis the choroid will be considered to be a thin layer of blood which rests on a "black" substrate. The substrate has the property of absorbing all of the light which is incident on it.

Consider a monochromatic beam of light which is incident upon the model choroid as shown in Figure A-2. In passing through a layer of blood of arbitrarily small thickness dx located a distance x below the front surface of the choroid some of the light will be transmitted, some absorbed, some scattered forward, and some scattered (or diffusely reflected) backward.

The change in intensity of the light transmitted in the forward direction is:

$$d I_T(x) = - \underbrace{\mu_c I_T dx}_{\text{absorption}} - \underbrace{\sigma_F I_T dx}_{\text{forward scattering}} - \underbrace{\sigma_B I_T dx}_{\text{backscattering}} \quad (\text{A-1})$$

The change in intensity of the light scattered in the forward direction is:

* Table A-I gives a list of symbols and abbreviations used.

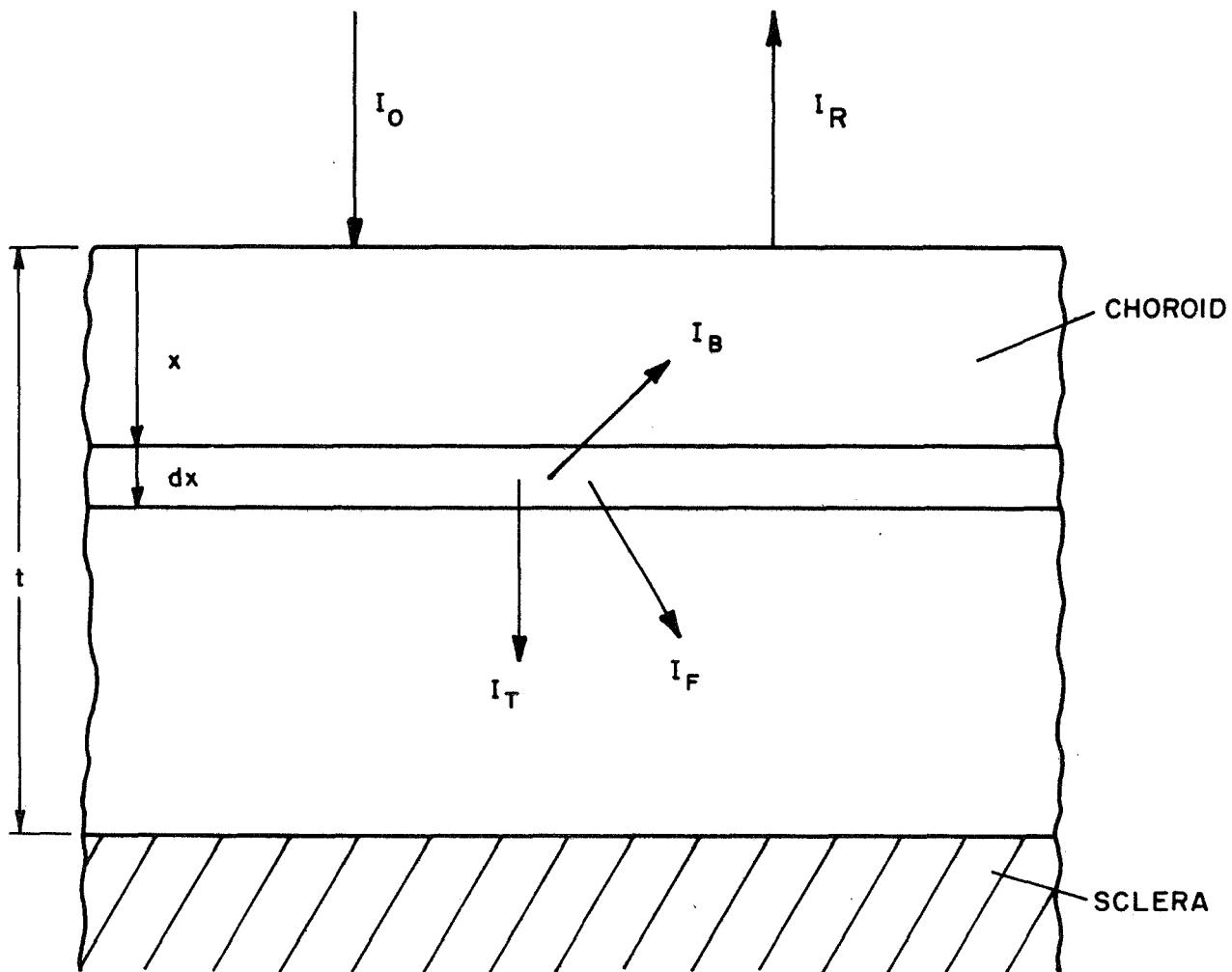


FIGURE A-2.
MODEL OF THE FUNDUS.

TABLE A-I

SYMBOLS

$I_O = I_O(\lambda)$	= intensity of light of wavelength λ incident upon the choroid.
$I_R = I_R(\lambda)$	= intensity of light of wavelength λ diffusely reflected from the choroid.
$I_T = I_T(x)$	= intensity of light transmitted in the forward direction at a distance x from the front surface of the choroid.
$I_F = I_F(x)$	= intensity of light scattered in the forward direction in passing through a layer of blood of thickness dx located at a distance x from the front surface of the choroid.
$I_B = I_B(x)$	= intensity of light scattered in the backward direction in passing through a layer of blood of thickness dx located at a distance x from the front surface of the choroid.
Hb	= Hemoglobin
HbO ₂	= Oxyhemoglobin
$c = c_{Hb} + c_{HbO_2}$	= Total hemoglobin concentration
μ	= molecular absorption coefficient of blood.
μ_{Hb}	= molecular absorption coefficient of hemoglobin.
μ_{HbO_2}	= molecular absorption coefficient of oxyhemoglobin.
σ_F	= scattering coefficient of blood in "forwards" direction.
σ_B	= scattering coefficient of blood in "backwards" direction.
t	= thickness of choroid

$$d I_F (x) = - \underbrace{\mu c I_F dx}_{\text{absorption}} + \underbrace{\sigma_F I_T dx}_{\text{forward scattering of transmitted beam}} - \underbrace{\sigma_B I_F dx}_{\text{back scattering}} + \underbrace{\sigma_B I_B dx}_{\text{forward scattering of light previously backscattered}} \quad (\text{A-2})$$

The change in intensity of light scattered in the backwards direction is:

$$- d I_B (x) = - \underbrace{\mu c I_B dx}_{\text{absorption}} + \underbrace{\sigma_B I_T dx}_{\text{back scattering of transmitted beam}} - \underbrace{\sigma_B I_B dx}_{\text{forward scattering}} + \underbrace{\sigma_B I_F dx}_{\text{backscattering of light previously forward scattered}} \quad (\text{A-3})$$

Equation (A-1) - (A-3) can be written to give

$$\frac{d I_T}{dx} = - (\mu c + \sigma_F + \sigma_B) I_T \quad (\text{A-4})$$

$$\frac{d I_F}{dx} = \sigma_F I_T - (\mu c + \sigma_B) I_F + \sigma_B I_B \quad (\text{A-5})$$

$$- \frac{d I_B}{dx} = \sigma_B I_T + \sigma_B I_F - (\mu c + \sigma_B) I_B \quad (\text{A-6})$$

Equations (A-4) - (A-6) form a set of three linearly independent first order differential equations in the three unknowns I_T , I_F , and I_B .

These equations have been solved to give the reflected intensity $I_R = I_B(0)$ subject to the boundary conditions of the problem ($I_B = 0$ at $x = t$ and $I_F = 0$ at $x = 0$). The expression for I_R which is obtained is

$$I_R = \frac{\sigma_B I_0}{\sigma_B + \mu c + q \coth(qt)} \quad (\text{A-7})$$

where

$$q = \sqrt{(\mu c)^2 + 2\mu c \sigma_B}$$

For $qt \gg 1$,

$$I_R \approx \frac{\sigma_B I_0}{\mu c + \sigma_B + \sqrt{(\mu c)^2 + 2\mu c \sigma_B}} \quad (\text{A-8})$$

which can be further simplified to

$$I_R \approx \frac{\sigma_B I_0}{2\mu c} \quad (\text{A-9})$$

since experimentally $\sigma_B \ll \mu c$. The backscattering coefficient, σ_B , is independent of the Hb/HbO₂ ratio to first order and is essentially a function of the size, shape, and concentration of blood cells. Equations (A-7), (A-8), and (A-9) agree with those of Longini and Zdrojkowski (1).

Using deBeer's law we can write that

$$\mu c = \mu_{\text{Hb}} c_{\text{Hb}} + \mu_{\text{HbO}_2} c_{\text{HbO}_2} \quad (\text{A-10})$$

Substituting equation (A-10) into equation (A-9) gives the result that

$$I_R = \frac{\sigma_B I_0}{2(\mu_{\text{Hb}} c_{\text{Hb}} + \mu_{\text{HbO}_2} c_{\text{HbO}_2})} \quad (\text{A-11})$$

Consider now the simultaneous reflection of two beams of light of wavelengths 650 nm and 805 nm from the choroid. Using equation (A-11)

we can then write that

$$I_R(650) = \frac{\sigma_B(650) I_O(650)}{2 [\mu_{Hb}(650) c_{Hb} + \mu_{HbO_2}(650) c_{HbO_2}]} \quad (A-12)$$

and

$$I_R(805) = \frac{\sigma_B(805) I_O(805)}{2 [\mu_{Hb}(805) c_{Hb} + \mu_{HbO_2}(805) c_{HbO_2}]} \\ = \frac{\sigma_B(805) I_O(805)}{2 [\mu_{Hb}(805) c]} \quad (A-13)$$

since 805 nm is an isobestic wavelength so that $\mu_{Hb}(805) = \mu_{HbO_2}(805)$; and $c = c_{Hb} + c_{HbO_2}$. Forming the ratio $I_R(805)/I_R(650)$ gives

$$\frac{I_R(805)}{I_R(650)} = \frac{\sigma_B(805)}{\sigma_B(650)} \cdot \frac{I_O(805)}{I_O(650)} \left[\frac{\mu_{Hb}(650)}{\mu_{Hb}(805)} (S_R) + \frac{\mu_{HbO_2}(650)}{\mu_{Hb}(805)} (1-S_R) \right] \quad (A-14)$$

where the oxygen saturation $S_R = \frac{c_{Hb}}{c_{Hb} + c_{HbO_2}}$.

Equation (A-14) can be solved for S_R to give

$$S_R = a \left[\frac{I_R(805)}{I_R(650)} \right] + b \quad (A-15)$$

where

$$a = - \frac{\sigma_B(650) I_O(650)}{\sigma_B(805) I_O(805)} \cdot \frac{\mu_{Hb}(805)}{\mu_{HbO_2}(650) - \mu_{Hb}(650)} \quad (A-16)$$

and

$$b = \frac{\mu_{HbO_2}(650)}{\mu_{HbO_2}(650) - \mu_{Hb}(650)} \quad (A-17)$$

Equation (A-15) gives a relationship between the measurable quantities $I_R(805)$ and $I_R(650)$ and the oxygen saturation S_R . It therefore provides us with a method of determining S_R by measuring the reflected intensities of light of wavelengths 805 and 650 nm from the choroid. The constants a and b are dependent only upon the known molecular absorption coefficients of Hb and HbO_2 , the incident light intensity, and the ratio of the back-scattering coefficients of blood at 650 nm and 805 nm.

Equation (A-15) has been experimentally verified by Polanyi and Hehir (2). Their data give the results that $a = -0.28$ and $b = +1.13$ for light of wavelengths 805 nm and 660 nm.

APPENDIX A - REFERENCES

1. Longini, R.L., and Zdrojkowski, R., IEEE Transactions on Bio-Medical Engineering, BME -15, No. 1, Jan. 1968.
2. Polanyi, M.L. and Hehir, R.M., Rev. Sci, Inst. 31: 401, 1960.

APPENDIX B

CALCULATION OF THE EYE OXIMETER SIGNAL TO NOISE RATIO

An analysis has been performed of the two-color eye oximeter to determine the anticipated signal-to-noise ratio (S/N) at the output of the photodiode and the relative light and signal levels at various points in the optical system. The analysis shows that a S/N of greater than 10^3 is anticipated using an FCS lamp for the light source and assuming that the light incident on the retina and the area measured by the photodetector covers the same 28° field of view.

Figure B-1 presents a diagram of the optical system. Table B-I presents a summary of the numerical results obtained. The discussion given below indicates the method and approximations used to obtain these results and provides references to the source literature used. Although the calculation is performed with respect to the FCS lamp and the HP-4204 diode used in the Eye Oximeter, modification to relate to other sources and detectors is straightforward. The calculation, which assumes that throughput is maximized, starts by calculating the radiant emittance of the FCS lamp in 10 nm bandwidths centered at 650 nm and 805 nm. The radiant flux in these two bands is then calculated and the losses to be expected for each of the optical components estimated. The S/N ratio at the output of the detector and the signal voltage at the pre-amp input are finally determined by using the published values for the photodetector parameters and the calculated radiant flux incident on the photodiode.

The radiant flux within a bandwidth of 10 nm centered at wavelength λ , $P_D(\lambda)$, which is incident upon the detector can be written as

$$P_D(\lambda) = P_Q(\lambda) \Pi_i T_i \quad (B-1)$$

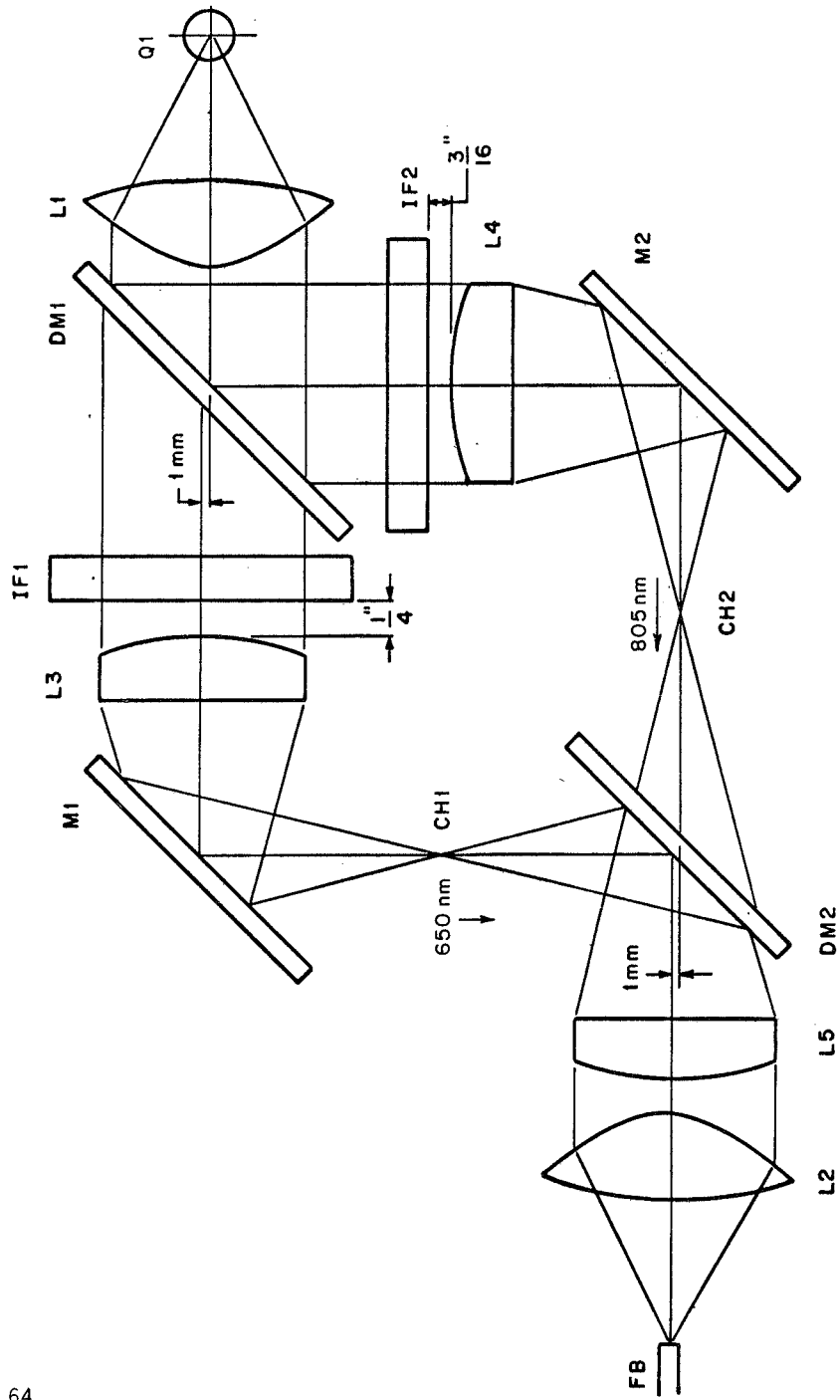


FIGURE B-1.
OPTICAL LAYOUT DIAGRAM OF DBLS.

TABLE B-I

SUMMARY OF RESULTS

<u>Calculation</u>	<u>At All Wavelengths</u>	<u>At 650 nm</u>	<u>At 805 nm</u>	<u>Units</u>
Radiant Emittance of FCS Lamp	219	1.0	1.4	Watts/cm ²
Radiant Flux, $P_Q(\lambda)$, From FCS Lamp		0.075	0.10	Watt
Collection Efficiency of Condensing Lens, T_o	0.135			
Transmission Coefficient of: Condensing & Exit Lenses, T_c	0.85			
DBLS, T_{DBLS}	0.25			
Fiber-optic Bundle, T_{FB}	0.4			
Fundus Camera to Eye, T_{FC}	0.3			
Eye, T_{eye}		2×10^{-3}	5×10^{-3}	
Fundus Camera to Detector, T_{det}	0.1			
Crossed Polarizers, T_p	0.15			
S/N at Preamp. Input		9×10^4	3×10^5	
Signal Voltage at Preamp. Input		0.03	0.1	Volt

where $P_Q(\lambda)$ is the radiant flux within a bandwidth of 10 nm centered at wavelength λ which is radiated from the source and the T_i 's are the transmission factors of the various parts of the optical system.

B.1 Radiant Flux Emitted By FCS Bulb, $P_Q(\lambda)$

The color temperature of the tungsten filament of the FCS lamp operated at 24 volts is 3200°K (Ref. 1). The temperature of a tungsten filament having this color temperature is 3100°K (Ref. 2). The FCS lamp, operated at 24 volts, can thus be assumed to radiate as a blackbody at a temperature of 3100°K corrected for the spectral emissivity of tungsten. The total radiant emittance of the FCS filament can then be calculated using the equation (Ref. 3)

$$W = \epsilon \sigma T^4 \quad (\text{B-2})$$

where ϵ is the emissivity of the tungsten surface, T is the temperature of the filament in $^\circ\text{K}$, σ is the Stefan-Boltzmann constant ($\sigma = 5.672 \times 10^{-12}$ for T in $^\circ\text{K}$ and W in watts/cm^2). Using an average of 0.42 for the emissivity of tungsten (Ref. 2) gives

$$W = \epsilon \sigma T^4 = 0.42 \times 5.672 \times 10^{-12} \times (3100)^4 = 219 \text{ watt/cm}^2 \quad (\text{B-3})$$

for the total radiant emittance of the FCS bulb. The radiant emittance, dW , within a bandwidth $d\lambda = 10 \text{ nm}$ centered at $\lambda = 650$ and 805 nm can be calculated using the equation

$$dW(\lambda) = W(\lambda) d\lambda = \frac{C_1 \lambda^{-5} d\lambda}{\exp(C_2/\lambda T) - 1} \quad (\text{B-4})$$

Using the values $\lambda = 650$ or 805 nm, $d\lambda = 10$ nm, $C_1 = 3.740 \times 10^{20}$, $C_2 = 1.4385 \times 10^7$, $T = 3100^\circ\text{K}$, $\epsilon(650) = 0.42$, and $\epsilon(805) = 0.40$ (Ref. 4) we obtain:

$$dW(650) = 1.05 \text{ watts/cm}^2 \quad (\text{B-5a})$$

and

$$dW(805) = 1.40 \text{ watts/cm}^2 \quad (\text{B-5b})$$

for the radiant emittance within the two desired spectral bands.

The filament of the FCS lamp is rectangular of nominal dimensions 2.9 mm x 5.8 mm. The maximum useful area of the filament (if only spherical lenses are used) is a circle of approximate radius 1.5 mm which has an area of $A = 7.1 \times 10^{-2} \text{ cm}^2$. The radiant flux of the FCS filament is then:

$$\Phi(650) = dW(650)A = 0.075 \text{ watt into a 10 nm bandwidth} \quad (\text{B-6a})$$

$$\Phi(805) = dW(805)A = 0.10 \text{ watt into a 10 nm bandwidth} \quad (\text{B-6b})$$

B.2 Collection Efficiency of Condensing System, T_o

The collection efficiency of a condensing system, T_o , can be defined as the amount of light collected by the condensing system divided by the total amount of light radiated by the source. Assuming that the FCS lamp radiates uniformly in all directions, we have;

$$T_o = \frac{\Omega}{4\pi} = \frac{d^2}{16f^2} \quad (\text{B-7})$$

where Ω is the solid angle subtended by the first condenser lens, L1, at the position of the filament, d is the diameter of L1, and f is the focal length of L1.

In the Eye Oximeter L1 has a diameter of 62 mm and a focal length of 42 mm so that we obtain a value of

$$T_o = \frac{d^2}{16f^2} = \frac{(62)^2}{16 \times (42)^2} = 0.135 \quad (\text{B-8})$$

B.3 Transmission of the Condensing and Exit Lenses, T_C

For an unpolarized beam of light incident upon a surface the intensity reflected, I_R , compared to the incident intensity, I_o , is given by (Ref. 5)

$$\frac{I_R}{I_o} = \frac{1}{2} \frac{\tan^2(\phi - \phi^1)}{\tan^2(\phi + \phi^1)} + \frac{1}{2} \frac{\sin^2(\phi - \phi^1)}{\sin^2(\phi + \phi^1)} \quad (\text{B-9})$$

where ϕ is the angle of incidence and ϕ^1 is the angle of refraction at the surface. If the incident beam is traveling in a medium of index of refraction n and the refracted beam in a medium of index n' then this equation reduces to

$$\left. \frac{I_R}{I_o} \right|_{\phi=0} = \left[\frac{n - n'}{n + n'} \right]^2 \quad (\text{B-10})$$

for normal incidence.

Throughout the analysis Equation (B-10) will be used to give the transmission factor for each optical interface although the general equation should more properly be used. The uncertainties in some of the other data used in this calculation are sufficiently large that using the exact equation for I_R/I_o is not warranted.

At a glass-air interface with $n = n(\text{air}) = 1$ and $n' = n(\text{glass}) = 1.5$ we obtain for the reflection loss, assuming normal incidence:

$$\frac{I_R}{I_o} = \left[\frac{n - n'}{n + n'} \right]^2 = \left[\frac{1 - 1.5}{1 + 1.5} \right]^2 = 0.04 \quad (\text{B-11})$$

The transmission factor for such an interface is then

$$T_{\text{glass-air}} = 1 - \frac{I_R}{I_O} = 0.96 \quad (\text{B-12})$$

The condensing and exit lenses, L1 and L2, have four interfaces and so the two lenses will have a combined transmission factor of

$$T_C = (0.96)^4 = 0.85. \quad (\text{B-13})$$

B.4 Transmission of the DBLS, T_{DBLS}

Each beam passes through 1 chopper aperture, 2 lenses, 1 dichroic mirror and 1 interference filter, and reflects from 1 first-surface mirror and 1 dichroic mirror. The transmission factors for the various components can be estimated as:

<u>Component</u>	<u>T_i</u>
2 lenses	$(0.96)^4 = 0.85$
1 first-surface mirror	0.96
1 chopper	0.75 when "on" (Ref. 6) 0.00 when "off"
1 interference filter	0.55 (Ref.7)
1 dichroic mirror (transmit)	0.85 (Ref.8)
1 dichroic mirror (reflect)	0.96 (Ref.8)

The total transmission factor for the DBLS is the product of these component factors or

$$T_{\text{DBLS}} = \prod_i T_i = 0.28. \quad (\text{B-14})$$

B.5 Transmission of the Fiber-optic Bundle, T_{FB}

The transmission of the fiber-optic bundle connecting the DBLS to the fundus camera has been measured to be

$$T_{\text{FB}} = 0.4.$$

B.6 Fundus Camera Transmission Coefficient, Source to Eye, T_{FC}

The transmission coefficient of the Fundus camera from the source to the eye has been measured to be

$$T_{FC} = 0.30 \quad (B-15)$$

B.7 Crossed Polarizer Transmission Coefficient, T_P

The two crossed polarizers which are put in the measuring beam to reduce the noise due to glare cause a further reduction in signal (but an increase in S/N) which has been measured to be

$$T_P = 0.15 \quad (B-16)$$

B.8 Transmission Coefficient of the Eye, T_{eye}

The transmission coefficient of the eye, T_{eye} can be written as;

$$T_{eye} = I_{out} / I_{incident} = T_{oc}^2 R_F K_1 K_2 \quad (B-17)$$

where T_{oc} is the transmission coefficient of the ocular media of the eye, R_F is the reflection coefficient of the fundus, K_1 is the ratio of the fundal area illuminated to that "observed" during the measurement, and K_2 is the ratio of the reflected light collected by the pupil of the eye to that emitted by the fundal area under observation.

The reflection losses from each of the optical interfaces of the eye can be calculated using Equation (B-10). The nominal index of refraction of the various ocular media are: $n(\text{cornea}) = 1.376$, $n(\text{aqueous humor}) = 1.336$,

$n(\text{lens}) = 1.386 - 1.406$ and $n(\text{vitreous humor}) = 1.337$.

The reflection loss ℓ_i at each ocular interface is then:

$$\ell_1 = \ell \text{ (air to cornea)} = \left(\frac{1.38 - 1.00}{1.38 + 1.00} \right)^2 = 0.026 \quad (\text{B-18a})$$

$$\ell_2 = \ell \text{ (cornea to aqueous)} = \left(\frac{1.336 - 1.376}{1.336 + 1.376} \right)^2 = 0.00022 \quad (\text{B-18b})$$

$$\ell_3 = \ell \text{ (aqueous to lens)} = \left(\frac{1.40 - 1.34}{1.40 + 1.34} \right)^2 = 0.00048 \quad (\text{B-18c})$$

$$\ell_4 = \ell \text{ (lens to vitreous)} = \left(\frac{1.34 - 1.40}{1.34 + 1.40} \right)^2 = 0.00048. \quad (\text{B-18d})$$

The transmission factor of the ocular elements of the eye is thus

$$T_{\text{oc}} = \prod_{i=1}^4 (\ell - \ell_i) = 0.97. \quad (\text{B-19})$$

This calculated value compares favorably with the measured value of 0.96 - 0.97 for human eyes (Ref. 9), indicating that little or no light is absorbed by the ocular elements of the eye. The reflection coefficient of the human fundus, R_F , has been measured by Brindley and Willmer (Ref. 10) over the range of 460 - 680 nm. Their data indicates that

$$R_F(650) \approx 2 \times 10^{-2} \quad (\text{B-20})$$

If we assume that the reflection coefficient of the sclera is the same at both 650 and 805 nm then we can estimate the reflection coefficient of the fundus at 805 nm by multiplying $R_F(650)$ by the ratio of the transmission coefficients T_F of the fundus at 805 and 650 nm, which can be obtained from the data of

Geeraets, et al. (Ref. 9). Thus,

$$R_F(805) \approx R_F(650) \times \left(\frac{T_F(805)}{T_F(650)} \right) = 2 \times 10^{-2} \times \left(\frac{48}{20} \right) \approx 5 \times 10^{-2} \quad (\text{B-21})$$

The factor K_1 can be written as;

$$K_1 = \frac{\text{fundal area illuminated}}{\text{fundal area "observed"}} = \left(\frac{\theta}{\gamma} \right)^2 \quad (\text{B-22})$$

where θ is the angle subtended by the observed fundal area at the pupil and γ is the fundal area irradiated by the incident beam. (For the unmodified Topcon Fundus Camera $\gamma = 28^\circ$.) If the light reflected from the entire illuminated fundal area is focused on the photodetector then $K_1 = 1$. (We will refer to this situation as 28-28 illumination.) If the field stop of the Fundus Monitoring Unit were closed down so that a fundal area less than 28° were measured equation (B-22) would be used to give the proper value of K_1 to use in the calculations. Table B-I would then have to be modified accordingly.

The factor K_2 can be calculated by assuming that the illuminated fundal area radiates as an extended diffuse source obeying Lambert's law. If θ_o is the angle subtended by a 5 mm pupil which is 22 mm from the radiating fundal area then K_2 can be written as,

$$K_2 = \frac{\int_0^{\theta_o} I_o \cos \theta \, d\theta}{\int_0^{\pi/2} I_o \cos \theta \, d\theta} = 0.114 \quad (\text{B-23})$$

Using the above values for $T_{oc,F}$, R_F , K_1 , and K_2 , the transmission factor of the

eye, T_{eye} , is given by

$$T_{eye}^{28-28}(650) = T_{oc}^2 R_F K_1 K_2 = (0.97)^2 \times 2 \times 10^{-2} \times 1 \times 0.11 = 2.2 \times 10^{-3} \quad (B-24)$$

for 28-28 fundal illumination.

The transmission coefficients for 805 nm are larger than those given in Equation (B-24) by a factor of $R_F(805)/R_F(650) = 2.5$.

B.9 Fundus Camera Transmission Coefficient, Eye to Detector, T_{det}

The transmission coefficient of the fundus camera and the collection efficiency of the detector are estimated to provide an "effective transmission factor" of

$$T_{det} = 0.1 \quad (B-25)$$

B.10 Radiant Flux Incident on Detector, $P_D(\lambda)$

The radiant flux incident on the detector is obtained by using Equation (B-1) to give

$$\begin{aligned} P_D(\lambda) &= P_Q(\lambda) \Pi T_i \\ &= P_Q(\lambda) \times T_o \times T_C \times T_{DBLS} \times T_{FC} \times T_{eye} \times T_{det} \times T_{FB} \times T_P \end{aligned} \quad (B-26)$$

Using the values calculated above for $P_Q(\lambda)$ and the T_i 's gives

$$P_D(650) = 8.6 \times 10^{-9} \text{ watts} \quad (B-27a)$$

$$P_D (805) = 29 \times 10^{-9} \text{ watts} \quad (\text{B-27b})$$

B.11 Signal-to-Noise Ratio, S/N, at Input to Preamplifier

The noise equivalent power of the HP 4204 PIN photodiode (which includes both thermal and shot noise) is 1×10^{-13} watt for a one Hz bandwidth and a 10^7 ohm load resistor (Ref. 11). The S/N for 28-28 illumination is then

$$S/N (650)^{28-28} = 8.6 \times 10^4 \quad (\text{B-28a})$$

$$S/N (805)^{28-28} = 29 \times 10^4 \quad (\text{B-28b})$$

B.12 Signal Level at Preamplifier Input

The sensitivity of the HP 4204 is (Ref. 12)

$$S(650) = 0.35 \mu\text{a}/\mu\text{w} \quad (\text{B-29a})$$

$$S(805) = 0.45 \mu\text{a}/\mu\text{w} \quad (\text{B-29b})$$

Using a 10^7 ohm load resistor and the values of $P_D(\lambda)$ from Equations (B-27a) and (B-27b) gives signal voltages of

$$V^{28-28}(650) = 3.0 \times 10^{-2} \text{ volts} \quad (\text{B-30a})$$

and

$$V^{28-28}(805) = 13 \times 10^{-2} \text{ volts} \quad (\text{B-30b})$$

APPENDIX B - REFERENCES

1. G.E. Drawing Number 281A-400, or G.E. Catalogs P8-67P or P6-113P-R.
2. Handbook of Chemistry and Physics . 48th edition, Chemical Rubber Publishing Co., p. E-164.
3. See, for example, Sears, F.W.; Optics, Addison-Wesley Publishing Co., 1949, p. 315 ff.
4. From an extrapolation of tabular data in the Handbook of Chemistry and Physics, Op.cit., p. E-154.
5. F.W, Sears, Op.cit., p.173.
6. Our measurements.
7. Oriel Optics Company Catalog.
8. Bausch and Lomb Multifilms Catalog 44-306, p.20.
9. Geeraets, W.J., et al.: Arch. of Opthal., 64: 606 (1960).
10. Brindley, G.S. and Willmer, E.N.: "The Reflection of Light from the Macular and Peripheral Fundus Oculi in Man." J. Physiol., 116: 350-356, 1952.
11. Hewlett-Packard PIN Photodiode Data Sheet, 15 Dec. 1967, HP 5082-4200 Series.

APPENDIX C
NEW TECHNOLOGY APPENDIX

"After a diligent review of the work performed under this contract,
no new innovation, discovery, improvement or invention was made."